AUGUST 2011

Ph.D. DISSERTATION

Identification and characterization of amyloid beta interacting proteins

Graduate School of Chosun University

Department of Bio-Materials

Md. Golam Sharoar

Identification and characterization of amyloid beta interacting proteins

아밀로이드베타 결합단백질의 확인과 특성분석

25th August 2011

Graduate School of Chosun University

Department of Bio-Materials

Md. Golam Sharoar

Identification and characterization of amyloid beta interacting proteins

Advisor: Prof. Il-Seon Park

This dissertation is submitted to the Graduate School of Chosun University in partial fulfillment of the requirements for the degree of Doctor of Philosophy in Science

April 2011

Graduate School of Chosun University

Department of Bio-Materials

Md. Golam Sharoar

This is to certify that the Ph.D. thesis of **Md. Golam Sharoar** has successfully met the dissertation requirements of Chosun University

Chairperson	:	Prof. Kyung Soo Ham	_____
Committee Member	:	Prof. Song Yub Shin	_____
Committee Member	:	Prof. Tae Hyoung Kim	_____
Committee Member	:	Prof. Il-Seon Park	_____
Committee Member	:	Prof. Takbum Ohn	_____

June 2011

Graduate School of Chosun University

CONTENTS

LIST OF FIGURES

초 록

아밀로이드베타 결합단백질의 확인과 특성분석

샤로아고람무하마드

지도교수: 박 일 선

조선대학교 대학원

생물신소재학과

베타-아밀로이드(Aβ)는 알츠하이머 질병의 주요 병인이다. 일반적으로 이 펩타이드는 세포의 내부 및 외부 과정을 통해 caspase를 활성화 시킴으로써 세포 사멸을 유도하는 것으로 알려져 있다. 그러나 본 연구에서는, 세포사멸 유도 단백질(caspase-9)과 Aβ의 새로운 상호 작용을 발견하였고, 이 상호작용으로 인해 일반적으로 세포 독성을 유발하는 것으로 알려져 있는 Aβ가 세포사멸을 억제 할 수 있음을 확인하였다. 세포 배양액에 첨가한 Aβ42는 stausporine에 의해 유도되는 DEVDase의 활성과 세포사멸을 억제하였다. 이것은 Aβ42 단백질이 Apaf-1 apoptosome의 형성을 억제하고 caspase-9과 -3의 활성화를 억제한 결과이다. 구체적으로 Aβ42는 pro-caspase-9과 결합하여 apoptosome 형성과 procaspase-9의 효소활성을 저해하고 이는 세포사멸 신호전달을 막는다. 그러나 이러한 현상은 CARD-deleted caspase-9에서는 발견할 수 없었다. 따라서 caspase-9의 CARD 도메인이 Aβ 의 상호작용에 매우 중요한 부분임을 확인하였다. 또한 세포사멸 억제효과는 epithelial HeLa와 osteosarcoma MG63 세포에서 현저하게 많이 나타나며, 상

대적으로 neuroblastoma SHSY5Y에서는 약하게 나타난다. 결과적으로, Aβ 펩타이드와 caspase-9은 상호작용 결과 inclusion body를 형성함으로써 세포사멸을 억제함을 확인하였다.

알츠하이머 질병은 Aβ의 축적에 의해 유발되는 질병이다. 그러나 본 연구에 의하면 말토오스 결합 단백질(MBP)는 Aβ 펩타이드의 축적을 막는다. MBP는 Aβ의 fibrillogenesis 초기단계에 결합하며, 펩타이드가 고비율로 존재할 때 fibril 형성을 효과적으로 억제한다. MBP는 Aβ 단량체 random coil에서 β - 시트 구조로의 펩타이드 전이를 차단하고 그 결과 다양한 Aβ 중간체가 형성되어 축적된다. 흥미롭게도, 축적된 oligomeric Aβ의 독성은 neuroblastoma SHSY5Y 세포에서 상대적으로 낮다. 결론으로, MBP는 Aβ fibrilogenesis의 nucleation 과정을 억제하고 펩타이드를 무독성 oligomeric 형태로 변형시킴으로써 Aβ 의 축적을 막는다.

또한, 천연 플라보노이드인 Keampferol - 3 – rhamnoside(K-3-rh)가 Aβ42의 축적과 세포독성에 미치는 영향을 결합 메커니즘을 통해 관찰하였다. 이 플라보노이드는 Aβ 세포 독성 억제 효과와 fibril 형성, 확장, 이차구조의 변형 등 항-amyloidogenic 효과가 있었다. 높은 농도의 K-3-rh 존재시 작은 oligomeric Aβ가 축적되는데 이로 인해 세포독성 유도 과정을 세포독성이 없는 과정으로 변형된다.

I. INTRODUCTION

I-1. Amyloid beta peptides

Amyloid beta (Aβ), a 4.5kD peptide, contain 39-42 amino acid residue derived by the sequential cleavage of β and γ scretases from amyloid precursor protein (APP) [1,2]. Generation of Aβ is closely related to the pathogenesis of a age related neurodegenerative disorder called Alzheimer's disease [3]. Alzheimer's disease (AD) is characterized by progressive and insidious neurodegeneration of the central nervous system which eventually leads to a gradual decline of cognitive function and dementia [4]. The principal neuropathological features of AD are the presence of neurofibrillary tangles and β-amyloid (Aβ) composed senile plaques [5,6] (Fig. 1A). The precursor of Aβ peptide, APP, is a large type 1 transmembrane protein of unknown function that is expressed in the heart, kidneys, lungs, spleen, intestine, and brain [7]. The majority of APP degrades in the endoplasmic reticulum and only a small fraction enters into the secretase cleavage pathway [1,2,6] (Fig. 1B).The first cleavage of APP by α- secretase results in the release of the large soluble ectodomain fragment α-APPs and retention of a C-terminal fragment C83 in the membrane which further cleaved by γ- secretase and releases a 3 kDa peptide, p3. While the cleavage of APP by β-secretase leads to the release of a soluble APP fragment β-APPs and the C-terminal fragment C99 (β-CTFs). Further processing of C99 by γ-secretase results in the generation of Aβ [7] (Fig. 1B). The differential cleavage by γ-secretase is one contributing factor for the formation Aβ with different C-termini. Among two most common alloforms of Aβ, Aβ40 ending at Val at 40 position and Aβ42 ending at Ala at 42 position, the longer form(Aβ42) is more prone to aggregate than the shorter form(Aβ40), and is the main constituent of senile plaques [8,9].

I-2. Aggregation of Aβ peptide and cytotoxicity

The amyloid cascade hypothesis suggests that Aβ aggregates are important etiology of AD [8]. Senile plaque of AD patent's brain mainly composed of fibrilar form of Aβ (fAβ) which explained as the peptide's polymers with cross β-sheet structure [10]. fAβ triggers a number of pathological conditions including tau hyperphosphorylation, which leads to neuronal dysfunction and degeneration [11]. Several lines of studies proposed that Aβ fibrilization follows nucleation-dependent aggregation which basically comprises two phases; nucleation and extension [12,13] (Fig. 1C). Nucleation phase is thermodynamically unfavorable and involves the formation of nucleus through a series of association of monomers [12]. Extension phase is thermodynamically favorable and accomplishes by the addition of monomers to the end of existing nucleus, leading to the rapid extension of fibrils [13]. Aβ fibrilization, however, precedes by multiple conformational changes including trimer, pentamer, or higher molecular weight complex formation, also known as Aβ -derived diffusible ligands (ADDLs) [14], oligomers composed of 15–20 monomers (AβOs) [15], protofibrils (string of oligomers) [16], and dodecameric oligomers Aβ *56[17] (Fig. 1D). These intermidiate speciece of Aβ fibrilogenesis pathway are designated collctively as "soluble Aβ" [18] which found in cerebrospinal fluid of AD patents [19]. The report also proposed that the Aβ oligomerization proceeds by association of monomers to form the initial pentamerhexamer units called paranuclei which further assembled to form beaded superstructures similar to early protofibrils [20] (Fig. 1E).

It was long assumed that Aβ has to be deposited in extracellular fibrilar

form to exert the toxicity [21,22]. The modified version of β-amyloid cascade hypothesis, however, suggests the possibility that Aβ-oligomers might contribute to AD pathogenesis rather than fibrillar amyloid deposits within the brain [23], which strongly supported by the evidence of soluble Aβ assembly in the brain of AD patent [19]. Now a number of studies have suggested that soluble, oligomeric, non-fibrillar forms of Aβ are more toxic than the mature fibrils, and a clear correlation have also shown between soluble Aβ levels and extent of synaptic loss and severity of cognitive impairments[24,25,26]. In a recent study, both soluble monomer and oligomer and insoluble amyloid plaque have been isolated from AD brain and the dimeric form defined as the smallest synaptotoxic species due to its severe impairment of synaptic plasticity in mouse hippocampus slice [27]. The monomer and plaque in insoluble form, on the other hand, have shown to devoid of toxicity [27] and in fact the neuroprotective effect have been suggested for the monomeric form of the peptide [28].

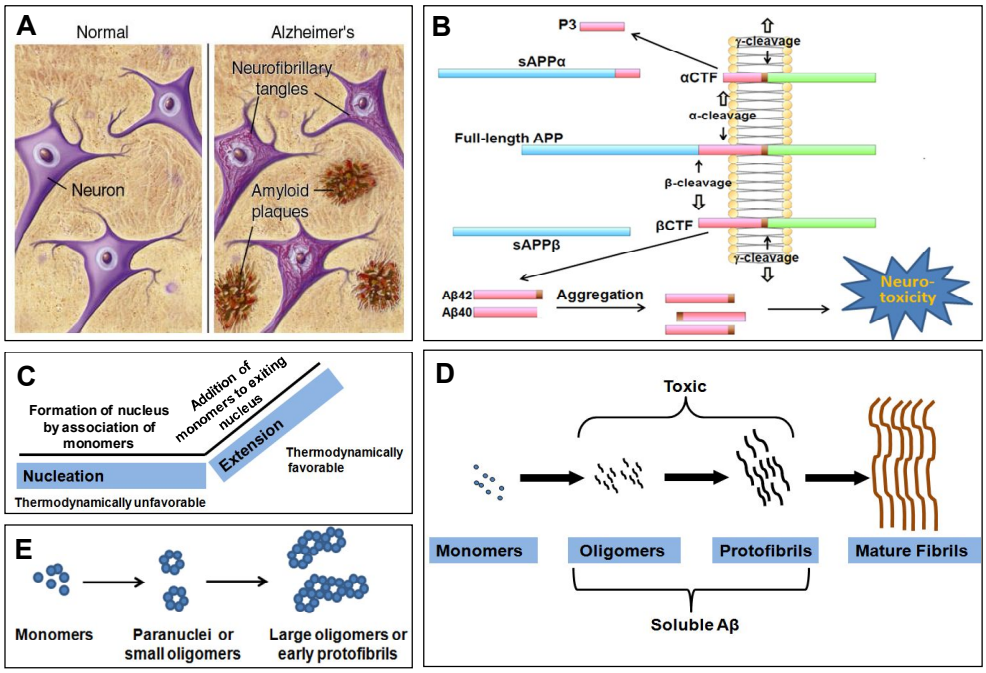

Fig. 1. Amyloid plaques, processing of amyloid precursor protein (APP) and aggregation of Aβ peptides. (A) In the brain of Alzheimer's patients, Aβ forms irresolvable clumps, known as amyloid plaques (Source: American Health Assistance Foundation). **(B)** Schematic diagram of APP processing (not drawn in proportion). Aβ peptides derived by the sequential cleavage of APP by β- and γ- secretases. **(C)** Nucleation dependent aggregation of Aβ peptides. **(D)** Schematic diagram of aggregation of Aβ peptides. The fibrilization of Aβ peptides proceeds by several conformational changes from monomers to oligomers, string of oligomers or protofibrils and then to mature fibrils. The oligomeric and protofibrilar intermediates are designated as soluble Aβ which found the most toxic forms of the peptides. **(E)** Aβ oligomerization process. Oligomerization proceeds by the assotiation of monomers to form pentahexamers paranuclei which further assembled to large oligomers.

I-3. Interaction Aβ with plasma membrane and receptor proteins

The mechanism of Aβs mediated cytotoxicity remains unclear. Due to its structural virtue, Aβs are able to bind to a variety of bio-molecules, including lipids, proteoglycans and proteins (Fig. 2). Several studies have shown a positive correlation between the binding of Aβ to the plasma membrane and the cytotoxicity induced by the peptide [29,30]. Aβ has been found to bind with a number of receptors or receptor related proteins such as low-density receptor-associated protein-1 [31], the α7-nicoti nic acetylcholine receptor [32], the p75 neurotrophin receptor [33] and the receptor for advanced glycation endproducts [34]. On the other hand report also proposed that Aβ binds to membrane lipids rather than binding to a specific receptor [35]. Membrane binding of Aβ has been reported as a necessary step to exert the toxicity by the peptide [36], while the interaction of Aβ with receptor associated protein (RAP) have been found to promote the cellular internalization of the peptide [37]. A recent study has been reported a new interaction of Aβ peptide with lipoprotein lipase (LPL) which promoted the membrane association and cellular uptake of the peptide [38].

The first order interaction of Aβ with cell membrane and receptors, however, facilitate the membrane permeability and internalization of the peptide. The binding of Aβ to membrane stimulates the Aβ aggregation due to the interaction between the anionic lipid and the peptide which enhances the structural transition of the peptide from random coils to β-sheet structure [39]. This enhancement of structural conversion along with increased membrane permeability leads to the formulation of the “channel hypothesis”, postulated on

the evidence of the formation of ion channel by Aβ peptides [40], and at least eight different ion channels have been characterized [41]. A report has been shown that the interaction of Aβs with the membrane leads to the formation of small oligomeric complexes which have been found to form multimeric channels with a central pore-like structure [42].

I-4. Cellular internalization of Aβ and interaction with intra-cellular proteins

The exogenous Aβs have been found to internalized and accumulated in neurons [43]. Several pathways have been proposed to mediate the event. Internalization via endocytosis and accumulation in the endosomal/lysosomal system have been suggested by an earlier study [44]. A recent *in vitro* study demonstrated that endocytosis of β-amyloid is regulated by a dynamin-dependent and RhoA-mediated pathway [45]. While, the contrasting evidence showed in an *in vivo* study, where the selective accumulation of β-amyloid in PC12 cells as well as cortical and hippocampal neurons found to occurs via a nonsaturable, energy independent, and nonendocytotic pathway [46]. The specific pathways involved in up taking and intracellular accumulation of Aβ peptides, however, remains unclear.

Aβ has been found to binds different molecules upon entering in to the cells (Fig. 2). One of these molecules is the Aβ-related death-inducing protein (AB-DIP) [47]. AB-DIP has been shown to activate and enhance cell death upon binding to Aβ [47]. A direct interaction between Aβ and mitochondria has also been shown in human neuroblastoma cells [48], which leads to the

transportation of the peptides in to the compartment by the translocase of the outer membrane (TOM40) and the translocase of the inner membrane (TIM22) [49]. The Aβ associated neurotoxic mechanism by mitochondrial dysfunction involved the interaction of the peptide with several mitochondrial proteins; one of those is ER amyloid β-peptide-binding protein (ERAB), also known as β-amyloid binding alcohol dehydrogenase (ABAD) [50]. ABAD assume to play a cyto-protective role in mitochondria by detoxifying aldehydes, such as, 4-hydroxy-2-nonenal (4-HNE), a cytotoxic hydroxyalkenal derived from lipid peroxides and a marker of oxidative stress [51]. The interaction of ABAD and Aβ leads to the dysfunction of mitochondria and generation of reactive oxygen species (ROS) by abrogating ABAD's 4-HNE detoxifying properties [51]. It has also been suggested that β-amyloid interacts with mitochondrial proteins from the membrane permeability transition pore (MPTP) [52]. A recent protein–protein interaction study suggested that the interaction between Aβ and adenine nucleotide translocase is stronger than that between Aβ and cyclophilin- D [53]. The complexes IV and V also reported as the targets for the peptides in human neuroblastoma cells [48]. The interaction of Aβ with mitochondrial membranes and mitochondrial proteins leads to mitochondria dysfunction through several events including the disturbance of membrane properties and calcium homeostasis, increasing ROS production, reducing oxidative phosphorylation and inducing apoptosis [54].

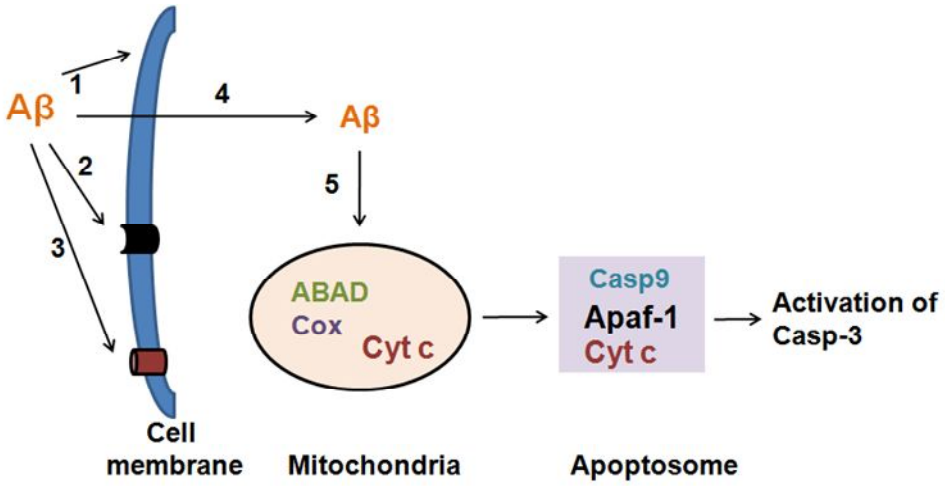

Fig. 2. Schematic diagram of cytotoxic effects of Aβ through interaction to membrane receptors and intracellular proteins. The cytotoxic effects of Aβ may results from the interaction of the peptide to several biomolecules; 1, direct interaction of Aβ peptide with cell membrane [30]; 2, binding to a specific receptor [32]; 3, forming a channel-like structure on cell membrane [41]; 4, interaction with unknown intracellular targets; 5, interaction with mitochondrial proteins such as ABAD [50] or cytochrome c oxidase [48].

I-5. Aβ induced apoptosis and cell death

The eventual consequence of Aβ interactions to extra- and intracellular proteins is the induction of cell death process through different biochemical events such as the activation of caspases [55,56,57], which has been a strong evidence for involvement of apoptosis in the death process [58]. Extensive evidence shows that apoptosis is involved in neuronal loss in AD [59,60]. The apoptosis, also known as programmed cell death, involves a series of biochemical events, both mitochondrial and non mitochondrial. The mitochondria-mediated apoptosis is characterized by the formation of apoptosome, a multiprotein complex that composed of cytochrome c released from mitochondria, Apaf-1, dATP and caspase-9 which becomes activated in the complex [61]. On the other hand, extracellular ligands such as TNFα, CD95 and Trail bind to the death receptors to form death inducing signaling complex (DISC) which activate caspase-8 in non mitochondrial receptor-mediated apoptosis [62]. Once apoptososme complex and DISC activate the initiator caspases, procaspase-9 and procaspase-8, respectively, it process the effector caspases such as caspases-3, -6 and -7 which are responsible for most of the downstream effects of apoptotic processes [63]. Studies have shown that Aβ induced the apoptosis process both *in vitro* [55] and *in vivo* [56] systems. Several hypotheses have been proposed for the mechanisms followed by Aβ to induce apoptosis. The mitochondrial release of apoptosis inducing factor (AIF) in cultured neurons [64] and the release of cytochrome c from isolated mitochondria [65] in presence of Aβ have been suggested, which subsequently initiates a caspase-independent apoptosis by causing DNA fragmentation and

chromatin condensation [64]. On the other hand, direct induction of apoptosis by Aβ has been reported by demonstrating the activation and processing of caspase-3 in rat cortial neurons after Aβ application [66]. The presence of caspase inhibitor has been found to block Aβ induced apoptosis without affecting the cell death by the peptide [66], which indicates different pathway(s) following by Aβ to kill the cells. The exact mechanism of Aβ induced apoptosis and its correlation with cell death, however, remains indistinct.

I-6. Inhibition of Aβ aggregation and cytotoxicity by proteins

Even after 100 years of discovery, the genetic, biochemical and biophysical elucidation of the origin of AD remains a complex and formidable challenge. The mechanism leading to cell death resulting from Aβ aggregation is beyond the clarification since the toxicity of processed Aβ peptide involve multiple pathways which may include a combination of apoptosis [67], ion dyshomeostasis [68], toxic radical [69] and complement formation [70]. Aggregations of soluble Aβ monomers to form toxic oligomers, protofibrillar and fibrillar species are considered to be the most critical step in the pathogenesis of the disease. The therapeutic strategy to inhibit this transition from monomer to toxic species, however, being practiced actively by numerous molecules that interact to Aβ [71]. Several intra- and extracellular chaperones have been found to regulate Aβ aggregation and toxicity. Identifying and utilizing proteins that interact to Aβ and inhibits its aggregation, however, might be potential to better understand the mechanism of the peptide's self-assembly and to develop therapeutic strategies.

Molecular chaperones are involved in several cellular processes including protein folding, degradation and subcellular trafficking [72]. Chaperone binding to the exposed hydrophobic stretch of amino acids mediates the flux between different protein conformations [73]. Several evidence such as, Aβ binding chaperones in cerebrospinal fluid [74], inhibition of Aβ amyloidogenesis by small heat shocks protein(sHsp) [75,76,77], interaction of Aβ peptide with several chaperone proteins and consequently suppression of cellular toxicity in transgenic *Caenorhabditis elegans* [78], suppression of *in vivo* Aβ toxicity by over expression of small chaperone [79] suggests the potentiality of molecular chaperones and chaperone like proteins as a therapeutic target for AD.

The consequences of Aβ and chaperones interaction have been reported to enrich or decrease aggregated species of the peptides. For example, apolipoprotein J (ApoJ), a senile plaque protein known as “clusterin or extracellular chaperone,” can interact with Aβ and influence the fibril formation [80], while the sHsp αB-crystallin prevents the amyloid fibril growth and at higher concentration accumulates toxic oligomers [77]. One the other hand, apolipoprotein E (Apo E) has been shown to have dual functions; binding to oligomeric Aβ by receptor mediated process and facilitating the deposition of the peptide as amyloid [81]. Whereas, the heat shock protein (Hsp) 90 and Hsp 70 shown to inhibit the aggregation of Aβ at earlier stage of fibrilogenesis [82]. The studies suggest that chaperones may regulates the Aβ aggregation and antagonize its biological effects but the consequence of interaction vary according to the types of chaperones.

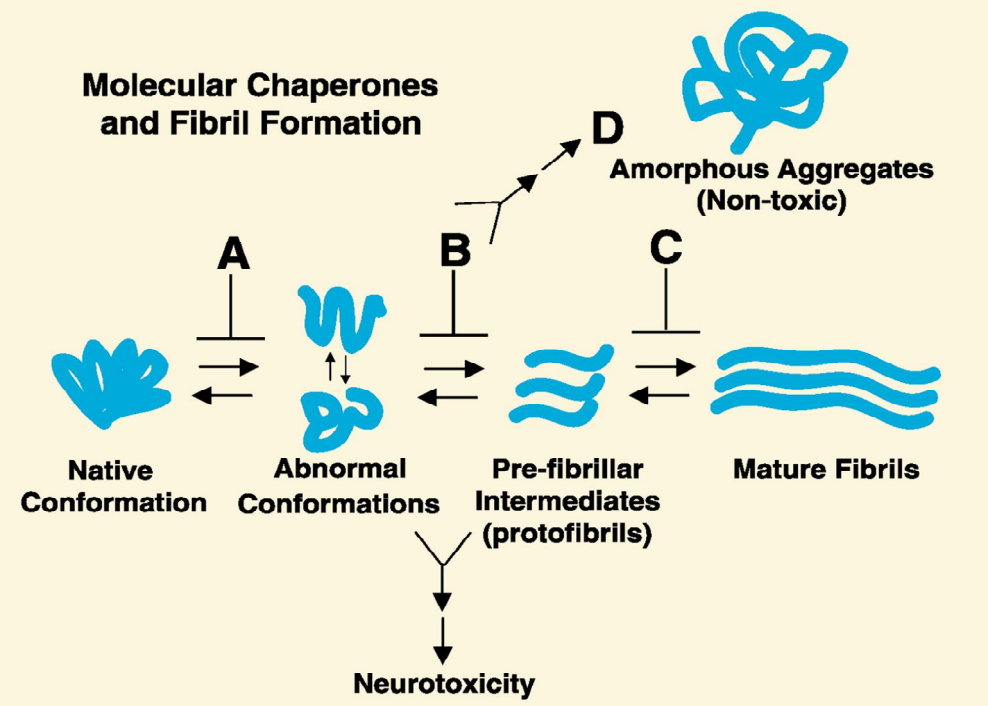

Fig. 3. A model for molecular chaperone suppression of Aβ mediated neurotoxicity (Source: Muchovski PJ. Protein misfolding, amyloid formation and neurodegeneration: a critical role for molecular chaperone. Neuron 2002;35:9-12). Molecular chaperones may suppress amyloid formation by participation in the pathways A, B, and C. Chaperones may also facilitated conversion of toxic intermediates into nontoxic amorphous aggregates (pathway D).

Though a number of proteins, particularly chaperones, have been identified as inhibitor of Aβ aggregation, its cytotoxic consequence is still confecting. The suppression of cytotoxic effects found *in vivo* by over expression of several proteins [78,83], but the *in vitro* studies showed that αB-crystalline [84], ApoE [85], α-antichymotrypsin [86] promoted the cytotoxicity. The concentrations of chaperones to exert inhibitory activity have been found very critical in some cases. For instance, small heat shock protein Hsp20 has been shown to inhibit Aβ toxicity at lower concentration, whereas it lost both aggregation and cytotoxic inhibitory properties at higher concentration [77]. While the reverse situation has been found in case of ApoJ [87]. The discrepancies have been explained as the pro-amyloidogenic property of chaperones may restrict in presence of substrate protein at a very large or small molar excess [87].

I-7. Inhibition of Aβ aggregation and cytotoxicity by chemicals

Several small molecules have been suggested as therapeutic agents and categorize according to their effectiveness to inhibit single or all steps of monomer > oligomer > fibril formation pathway [88]. Among the Aβ interacting small molecules, curcumin is one of the most attractive compound to the scientists due to its direct capability to bind with small Aβ species, to block aggregation and fibril formation and to disaggregates mature fibrils both *in vitro* and *in vivo* [89] conditions. The sulfonate dye Congo red and its derivatives[90] and thioflavin T(ThT) [91] were also reported to bind and stained amyloid in tissue section. These two dyes become popular and classic reagent to determine characteristic β-sheet mediated fibrilization. The notable point of the

studies regarding small molecule inhibitor of Aβ peptide is the most of reported inhibitors are structurally similar to Congo red and ThT, in that they are planar and aromatic.

The well-known role of aromatic stacking in processes of self assembly in chemistry and biochemistry [92] and the notable amount of aromatic residues in many amyloid related proteins and peptides [93,94] suggests that stacking of aromatic residues may involve in the assembly process of amyloidogenesis. The hypothesis have been proven by elucidating the strong effects of aromatic interaction on amyloidogenic propensity by protein folding modeling [95]. While, a mechanistic approach based on structural similarity of Aβ aggregation inhibitors have been suggested that all efficient inhibitor composed of at least two phenolic rings with two to six atom linkers, and a minimum number of three OH groups on the aromatic rings [96].

The flavonoids, found ubiquitously in plants, are the most common polyphenolic compounds group in human diet form [97]. This group of compounds have several beneficial effects on human health such as anti-oxidant [98], anti-allergic, anti-cancer and anti-inflammatory [99] and anti-microbial [100] activities. Flavonoids are also reported to decrease the risk of age related dementia [101]. The extensive studies on *Ginkgo biloba* extracts HE208 [102] and EGb 761[103] indicated that the flavonoids molecules are essentials for anti-amyloidogenic and anti-apoptotic activity in neural cells. Several isolated flavonoids such as myricetin, quercetin, kaempferol, morin, catechin, baicalein are now being described as anti-fibrillogenic and fibril-destablizing molecules but very few of them are found to be cyto-protective [104,105,106]. The mechanism of Aβ aggregation and its correlation to cytotoxic effects, however, remains to be elucidated.

Outlines of Thesis:

The thesis focused on the interactions of Aβ peptide with an intracellular and an extracellular proteins and its consequences. The initial part presents a new interaction mechanism of Aβ peptide with a protein involved in programmed cell death process. The later portions deal with the modulation of Aβ42 non-toxic aggregates using an extracellular protein and a polyphenolic compound, which found to interact with the peptide. The rationale of these studies is summarized below.

1. A novel interaction between Aβ42 and caspase-9 has been outline and anti-apoptotic function of Aβ42 peptide has been elucidated. The essential part of the protein for interaction has been identified and the consequent of the interaction has been illustrated. The inhibitory effect of the peptide on activation and activity of caspases have been analyzed.
2. A comprehensive study has been carried out to better understand the Aβ42 aggregation mechanism and its cytotoxic effect. An extra cellular protein has been identified to interact with Aβ and utilized to alter the assembly pathway of the peptide. The cytotoxic effects of the modulated species have been scrutinized.
3. A flavonoid has been employed to inhibit the toxicity and aggregation of Aβ42 peptide. The consequent of the inhibition, the accumulated intermediate Aβ species, has been examined and characterized.

II. MATERIALS AND METHODS

II-1. Materials

Fetal Bovine Serum (FBS) was purchased from Life Technology Inc. (Grand Island, USA). Dulbecco's modified Eagles medium, Ham's F 12 (1:1) (DMEM/F-12) and high glucose (DMEM/HG) were obtained from Welgene (Daegu, Korea). Caspase-9, caspase-8 and caspase-3 substrate, N-acetyl Leu-Glu-His-Asp-amino methyl coumarin (Ac-LEHD-AMC), Ac-IETD-AMC and Ac-DEVD-AMC, respectively, were from A.G. Scientific Inc. (San Diego, USA), Caspase inhibitor Z-VAD-FMK from Alexis (Lausen, Switzerland). Ni-NTA column were purchased from Amersham Biosciences (Piscataway, USA). Western blotting detection kit (WEST-ZOL plus) was from iNtron Biotechnology (Gyeonggi-do, Korea). Phosphate buffer saline (PBS) purchased from Amresco (Solon, USA). Monoclonal anti-Aβ antibody 6E10 was acquired from Signet Laboratories (Dedham, USA), anti-caspase-9 from MBL (Naka-ku Nagoya, Japan), anti-caspase-9(p10) and anti-caspase-3 from SantaCruz Biotechnology (California, USA), anti-caspae-8 from Cell Signalling Technology (Massachusetts, USA), anti-Apaf-1 and anti-Cytochrome C from AB Frontiers (Seoul, Korea), anti-DFF45 from BD Transduction Laboratory (San Diego, USA) and anti-Bid developed in laboratory. Polyclonal antibody anti-caspase-9(p10) obtained from Santacruz Biotechnology, urea was from USB chemicals, acetonitrile was from Merck (Darmstadt, Germany). All other chemicals were obtained from Sigma (St. Louis, USA), unless otherwise stated.

II-2. Preparation of amyloid beta

Amyloid beta peptides were expressed in *E. coli* as fusion proteins and purified as described before [107]. The purified peptides were solubilized in 100% 1,1,1,3,3,3,-hexafluoro-2-propanol, and dried under nitrogen flow and subsequently, under vacuum for 30 min. The peptide aliquots were stored at –20 °C until use. Immediately before use, the peptides were dissolved in 0.1% NH_4OH at a concentration of 2 mg/ml followed by bath sonication for 10 min at 4 ^{o}C. The solution was diluted at the desired concentration with PBS. Aβ42 oligomers were prepared as described earlier [108] with little modification. Briefly, peptides were diluted in cell culture media at 100 μM concentration, vortexed for 30 seconds and incubated at 4 °C for 12 h. The peptide solution then diluted to the desired concentrations. To make fibrils, Aβ42 (100 μM) was incubated in presence of 0.02% sodium azide in PBS at 37 °C for 4 days. The samples were centrifuged at 16000 x g for 30 min. Pellet fraction (fibrils) was washed three times with PBS. Fibrils were sonicated for 10 min, quantified by Bradford method and used immediately or stored at –80 °C.

II-3. Cell Culture and cell death assay

Human neuroblastoma SH-SY5Y was cultured in Dulbecco's Modified Eagles medium and Ham's F12 (1:1), while epithelial HeLa and ostieosarcoma MG63 cells were cultured in Dulbecco's Modified Eagles medium (high glucose) , both supplemented with 10% (v/v) fetal bovine serum (FBS) and 1% antibiotics, at 37 °C under 5% CO_2. Cells were seeded at a density of 20,000

cells/well in 96-well plates (Nunc, Denmark) and incubated for 24 h. The media were replaced with serum-free one and cells were further cultured for 12 h. To measure the cell death, cells were treated with indicated concentrations of Aβ and/or STS or Aβ in presence of MBP or flavonoid(s) for indicated times. Cell viability was assessed by MTT reduction assay. Briefly, 20 μl of 5 mg/ml MTT solution in PBS was added to each well and incubated for 2 h. Then, 100 μl of solubilization buffer [20% SDS solution in 50% (v/v) DMF (pH 4.7)] was added to each well. The absorbance was recorded after 12-16 h at 570 nm using micro plate reader Spectra Max 190 (Molecular Devices, CA, USA).

II-4. Measurement of DEVDase activity

DEVDase activity was measured as described earlier [109]. Briefly, treated cells were washed twice with ice-cold phosphate-buffer saline (PBS). Then, 40 μl of buffer containing 20 mM Hepes-NaOH, pH 7.0, 1 mM EDTA, 1 mM EGTA, 20 mM NaCl, 0.25% Triton X-100, 1 mM dithiothreitol (DTT), 1 mM phenylmethanesulphonylchloride (PMSF), 10 μg/ml leupeptin, 5 μg/ml pepstatin A, 2 μg/ml aprotinin, 25 μg/ml ALLN was added into each well and incubated on ice for 20 min. Caspase assay buffer(CAB) (final 20 mM Hepes-NaOH, pH 7.0, 20 mM NaCl, 1.5 mM $MgCl_2$, 1 mM EDTA, 1 mM EGTA and 10 mM DTT) was added and the release of AMC was monitored for 2 h in 2 minute interval with final 10 μM DEVD-AMC at excitation and emission wavelengths of 360 nm and 480 nm respectively, using micro plate spectofluoremeter (Molecular Devices, CA, USA). The results were expressed as a slope of total readings verses time.

II-5. Preparation of cell extract and cell free system

To prepare the cell extract, harvested cells were washed with ice-cold PBS, resuspended in buffer A (20 mM HEPES-KOH, pH 7.5, 0.5 mM EDTA, 0.5 mM EGTA, 10 mM KCl, 1 mM β-mercaptoethanol, 0.1 mM PMSF, 10 μg/ml leupeptin, 5 μg/ml pepstatin A, 2 μg/ml aprotinin, 25 μg/ml ALLN) and dounce-homogenized with 40-50 strokes. Supernatant was obtained by centrifugation at 17,000 x g for 1h and used immediately or stored at -80 °C.

In vitro apoptosis was induced by incubating the extract (100 μg) prepared from healthy or Aβ treated cell with 1 mM dATP and 0-10 μM cytochrome c or 1μg recombinant caspase-9 in buffer containing 20 mM HEPES-NaOH, pH 7.0, 20mM NaCl, 1 mM EDTA, 1 mM EGTA, 1.5 mM $MgCl_2$, 5 mM DTT for 1 h at 30 °C. To check the effects of Aβ in in cell free system, healthy cell extract was incubated with 1mM dATP and 1uM cytochrome c in presence of indicated concentrations of Aβ. The samples were then subjected to DEVDase activity measurement or western blotting. For the analysis of apoptosome assembly, the extract (900 μg) was reacted with 1 mM dATP and 6.67μg/ml cytochrome c for 1 h at 30 °C in same buffer.

II-6. Analysis of cytochrome c release

Cells were harvested, washed with ice-cold PBS and resuspended in digitonin buffer (75 mM NaCl, 1 mM NaH_2PO_4, 8 mM Na_2HPO_4, 250 mM sucrose, 190 μg/ml digitonin). After 5 min on ice, cells were spun for 5 min at 14,000 rpm at 4 °C in a microcentrifuge. Supernatants were transferred to fresh

tubes and the pellets were resuspended in buffer containing 25 mM Tris-HCl, pH 8.0, 1% Triton X-100. Equal amount of proteins from each sample were subjected to sodium dodecylsulfate-polyacrylamide gel electrophoresis (SDS-PAGE) and western blotting.

II-7. Western blot analysis

Cells were harvested, washed with ice-cold PBS and resuspended in buffer B (50 mM Tris-HCl, pH 8.0, 150 mM NaCl, 1% Triton X-100, 5 mM EDTA, 5 mM EGTA, 1 mM PMSF, 10 μg/ml leupeptin, 2 μg/ml pepstatin A and 2 μg/ml aprotinin) for 20 min on ice. The extract was obtained by centrifugation at 14,000 rpm at 4 °C for 15 min. The amount of protein was measured through Bradford assay. Equal amounts of proteins were separated on 12-15% SDS-PAGE and transferred on to a PVDF membrane. The membrane was immunoprobed with primary antibodies and horseradish peroxidase-conjuated secondary antibodies. The blots were visualized using West-Zol plus reagent (iNtron Biotechnology Inc, Seoul, Korea).

II-8. Chromatographic analysis of apoptosome assembly

Size exclusion chromatoghraphy was performed as described earlier [109]. Briefly, after Aβ and/or STS treatment, the cell extract was prepared in buffer C (20 mM HEPES-KOH, pH 7.5, 10 mM KCl, 1 mM EDTA, 1 mM EGTA, 2.5 mM $MgCl_2$, 2 mM DTT, 0.1% CHAPS, 10% glycerol, 0.1 mM PMSF, 10 μg/ml leupeptin, 5 μg/ml pepstatin A, 2 μg/ml aprotinin, 25 μg/ml ALLN) using

dounce-homogenizer. The cell extract (900μg - 2 mg) was loaded onto a Superose 6 HR (10/30) column (Amersham pharmacia biotech) pre-equilibrated with buffer C containing 50 mM KCl and proteins were eluted from the column at a flow rate of 0.2 ml/min and 0.5 ml fractions were collected. From each of the 0.5 ml fractions, appropriate fractions were concentrated in microcon (Millipore) concentrators (10 kDa cut-off) and analyzed by SDS-PAGE; followed by immunoblot analysis. The column was calibrated with calibration kits from Amersham pharmacia biotech, including thyroglobulin (669 kDa), ferritin (440 kDa), catalase (232 kDa), and aldolase (158 kDa).

II-9. Immunoprecipitation

Cell extracts, prepared in buffer D (50mM Tris-Cl, pH 7.4, 150 mM NaCl, 1 mM EDTA, 1 mM EGTA, 0.25%NP-40, 50Mm NaF, 0.1mM Na_3VO_4, 1mM DTT, 0.1mM PMSF, 10 g/ml leupeptin, 5 g/ml pepstatin A, 2 g/ml aprotinin, 25 g/ml ALLN), were diluted to 0.5mg/ml and cleared with 80μl protein A Sepharose beads(Amersham Biosciences, Uppsala, Sweden) at 4^{o}C for 1h. The indicated antibodies were then added to 100-500μg pre-cleared cell extract (final volume 1ml) and incubated at 4^{o}C over night with rotor agitation. Next, 10-50μl of beads were added to each sample and incubated at 4^{o}C for 2h. Beads were precipitate by centrifuging at 13000rpm at 4 ^{o}C for 5 min and washed 3 times with PBS. Fifteen μl 2X SDS loading buffer was added to the beads, boiled for 5 min and centrifuged at 13000rpm for 10 min. The obtained supernatants were then analyzed by SDS-PAGE and immunoblotting.

II-10. Immuno cytochemistry

HeLa cells were seeded in 12 wells plate at 70% confluency, cultured for 24h and further incubated for 12h in serum free medium and then treated without or with 20μM Aβ twice, and/or with STS. Harvested cells were fixed in methanol at -20^{o}C and permeabilized by 0.3% Triton X-100. After blocking with 0.1% BSA overnight, mouse anti amyloid beta (6E10) and rabbit anti caspase-9 antibodies (dilution, 1:100) were added and incubated overnight at 4^{o}C. After washing with PBS, Alexa-Fluor-488-conjugated chicken anti-mouse IgG and Alexa-Fluor-543-conjugated chicken anti-rabbit IgG antibodies (dilution, 1:200) were treated for 2h at room temperature followed by PBS washing. Nuclei were stained with DAPI in Vectashield mounting medium (Vector Laboratories, California, USA) and Confocal images were obtained with a Carl Zeiss LSM510 microscope (Jena, Germany) using the vendor-provided software (LSM510).

II-11. Immuno histochemistry

Desiccated brain tissue of cortex area, taken from the human Swedish mutant amyloid precursor protein (huAPP695.K670N/M671L) transgenic Tg2576 mice [110] and their littermate at the age of 8 month, were blocked with OCT cryo embedding media and 12 μm thick frozen brain sections were prepared by freezed microtome. The section were fixed with 98% methanol, permeabelized with 0.3% Triton X-100 and then blocked with 0.1% BSA in phosphate-buffered saline (pH 7.4) for 2h. After co-incubation with rabbit anti caspase-9 antibody (dilution, 1:100) and mouse anti amyloid beta (6E10)

antibody (1:100) overnight, the sections were washed 3 times with PBS. The samples were then reacted with Alexa Fluor 488 and Alexa Fluor 553 conjugated secondary antibodies (1:200). All stained samples were mounted using a mounting medium and fluorescence signals were imaged using Carl Zeiss LSM510 microscope.

II-12. Production of recombinant caspases

Recombinant caspases were purified as described previously [109,111]. Briefly, procaspase-9 (triple mutant at E306A, D315A and D330A), active caspase-9 (wild type), and caspase-9 lacking caspase recruitment domain (ΔCARD) cloned in pET28 vector were over expressed in pLysS *E. coli* strain. The caspases were purified by two successive chromatographic procedures. Initially, bacterial cell lysates prepared by sonication and centrifugation at 20 000 rpm for 1 h in buffer contain 20mM Tris-HCl, pH 8.0, 10mM NaCl, 0.1mM EDTA, 0.1mM PMSF, 1mM β-mercaptoethanol. The supernatant was loaded onto a Ni-NTA column (Qiagen) pre equlibriate with buffer contain 20mM Tris-HCl, pH 8.0, 10mM NaCl, 1mM β-mercaptoethanol, 10% glyceroland, eluted with same buffer supplemented with 250mM imidazole. The active fractions were diluted and applied to a HiTrapQ sepharose column (Amersham Pharmacia Biotech) equilibrated with buffer contain 20mM HEPES-NaOH, pH 7.5, 10mM NaCl, 0.1mM EDTA, 1mM DTT, 10% glycerol and eluted with 1–400mM NaCl gradient. The purified proteins were dialyzed against 20 mM Hepes (pH 7.5), 10 mM NaCl, 1 mM EDTA, 2 mM DTT, and 10% glycerol, and the aliquots were saved at -80^{o} C before use.

II-13. Binding assay with purified proteins

Ten μg of purified caspases (procaspase-9, caspase-9 and ΔCARD) were incubated with or without 20 μM Aβ42 for 1 h at 30 ^{o}C. Each reaction mixture was then subjected to gel filtration chromatography with a flow rate of 0.2 ml/min and 0.5 ml fractions were collected. The fractions were analyzed by immunoblot analysis for caspase-9 and Aβ.

II-14. Measurement of purified caspase activity using synthetic substrates

The activities of 1 μg of purified procaspase-9, caspase-9 and ΔCARD caspse-9 were measured in absence or presence of indicated amount of Aβ42 in caspase assay buffer (pH 7.0) using 50 μM Ac-LEHD-AMC. To check the apoptosome activity, 40 μl of 1.5 ml pooled fractions partially purified from the cell extract (2 mg) treated with 1 mM dATP and 1 μM cytochrome c using the size exclusion chromatography was incubated with Aβ42 at the indicated concentrations and their activities were assayed using 50 μM LEHD-AMC as a substrate, The fluorescence of the AMC release from the substrates was measured as described above.

II-15. Purification of MBP

Recombinant protein was purified from *E. coli* BL21 (DE3) pLysS. The cells containing recombinant MBP gene were grown to OD_{600} of ~ 0.6 followed

by induction with 0.4 mM IPTG for 4 h at 37^{o}C. The cells were harvested and lysed in buffer containing 20 mM Tris-Cl [pH 8.0], 10 mM NaCl, 0.1 mM PMSF, 0.1 mM EDTA, and 1 mM β-mercaptoethanol. The supernatants was obtained after centrifugation of the lysate at 18,000 rpm for 1 h were applied to Ni-NTA column pre equilibrated with buffer contain 20 mM HEPES-NaoH [pH 7.5], 150 mM NaCl, 10% glycerol and 1 mM β- mercaptoethanol and eluted with same buffer containing 250 mM imidazole. The aliquots of the purified protein were stored at -80 °C until use after being dialyzed against buffer B (20 mM HEPES [pH 7.5], 150 mM NaCl, and 20% glycerol). The purity of the purified protein was confirmed by SDS-PAGE analysis.

II-16. Th T assays

For initial fibrilogenesis assay, Aβ42 alone or with MBP were incubated in PBS at 37 °C for 12h and 20 μl from each reaction were mixed with 80 μl of 5μM ThT in PBS solution. Fluorescence was measured on microplate spectrofluorometer Gemini-XS (Molecular Devices CA, USA) using excitation at 440 nm and emission at 490 nm. For polymerization, assay, Aβ42 (20 μM) was incubated in PBS at 37 °C in presence of MBP or K-3-rh in a final volume of 30 μl without shaking. Tweenty μl from each reaction was mixed with 80 μl of 5 μM ThT in PBS solution and fluorescence was measured. Thioflavin-T fluorescence representing the characteristic sigmoidal curve was plotted as common logarithms in equation $\log\left[F(t)/A - F(t)\right] = at + b$ where t is the reaction time, $F(t)$ is the fluorescence as a function of time, A is tentatively

determined as $F(\infty)$, and a and b are the slope and $y-$ intercept, respectively [112]. Differentiating above equation by t and subsequent rearrangement produced a logistic equation, $F'(t) = BF(t)[A - F(t)]$, where, $B = a \ln 10\, A/2$, and $F'(t)$ represents rate of fluorescence increase at a given time. When $F(t) = A/2$, $F(t)/A - F(t) = 1$ and $F'(t)$ reaches its maximum. This time point was referred as $t/2$ [112]. For Aβ42 fiber extension assay, fresh Aβ42 (20 μM) was incubated with preformed Aβ42 fibril (1.1 μM) in presence of varying concentration of MBP or K-3-rh. For fibril destabilization assay, preformed Aβ42 fibrils (20 μM) were incubated in presence of varying concentration of K-3-rh.

II-17. Circular dichroism (CD) spectroscopy

Aβ42 (20 μM) was incubated in PBS at 37 °C either alone or presence of MBP (0.4 μM) or K-3-rh (20 μM) for 0, 12 or 24 h. CD spectra [113] were recorded with a 1-mm path length cuvette at 0.5 nm intervals between 190 nm and 250 nm at 1 nm resolution with a scan rate of 50 nm/min using a Jasco Sectropolarimeter (Jasco Co., Tokyo, Japan) at 25 °C. Average was taken from five scan for each sample. Aβ spectra were obtained by subtracting buffer background. Background spectra given by alone MBP or K-3-rh in identical conditions were subtracted from Aβ samples incubated in presence of MBP or K-3-rh. The corrected, averaged spectra were smoothed using means-movement algorithm in Jasco spectra analysis program.

II-18. Transmission Electron Microscopy (TEM)

Aβ42 (20μM) either alone or in presence MBP or K-3-rh was incubated in PBS at 37 °C for 12 h and 24h. Five μl of sample was adsorbed on Formvar-coated 200-mesh nickel grids for 30 min and extra solution was wiped-out [114]. The grids were negatively stained with 2% uranyl acetate for 1 min, washed with distilled water for at least three times. The samples were then analyzed with transmission electron microscopy (Hitachi, Japan) at an accelerating voltage of 80 kV at magnification of 40,000x

II-19. Detection of Aβ structural species by immunoblotting

Aβ42 was incubated in PBS at 37 °C with varying amounts of MBP or K-3-rh. Crosslinking of the peptide in the reaction mixture was carried out as described before, with slight modification [115]. Briefly, at the end of the reaction the samples were incubated with 0.01% glutaraldehyde in PBS for 10 min before being subjected to 16 % SDS-PAGE. Subsequently, the peptide was transferred to polyvinylidene difluoride (PVDF) membrane and hybridized with anti-Aβ antibody 6E10 (1:10,000). Then, the blots were incubated with horseradish peroxidase-conjugated Ig anti-mouse antibody (1:10,000) for 1 h at room temperature and developed using West-zol plus kit.

III. RESULTS AND DISCUSSION

III-1. Aβ inhibits mitochondria mediated apoptosis by interacting with procaspase-9

III-1-1. Aβ42 induced cell death are independent of DEVDase activity

Although a central role of the amyloid β (Aβ) in Alzheimer's disease (AD) is generally accepted, how the peptide leads to the neurodegeneration as well as the underlying pathology associated with AD is largely unknown. Involvement of apoptosis in the process has been suggested, because caspases are activated upon the administration of the peptide to cells [65,66]. The consistent results also observed in the present study for activation of DEVDase (mainly activity of caspase-3) in different cells treated with Aβ42 under the variable experimental conditions (Fig. 4A-C). Relatively less DEVDase activity was observed in epithelial HeLa (Fig. 4C) than neuroblastoma SH-SY5Y (Fig. 4A) and osteosarcoma MG63 (Fig. 4B) cells. Oligomeric Aβ42 induce comparatively more enzymatic activity than monomeric or fibrilar forms. Surprisingly, higher enzymatic activity was observed at a certain condition rather than dose dependent effects in SH-SY5Y and MG63 cells (Fig. 4 A and B).

The correlation of DEVDase activity and cell death induced by the oligomeric peptide was investigated by employing 3-(4,5-dimethylthiazol-2-yl)-2,5-diphenyl tetrazolium bromide (MTT) reduction assay in presence of a pan-

caspase inhibitor, z-VAD-fmk. Oligomeric Aβ42 cause the MTT reduction in dose dependent manner in SH-SY5Y (Fig. 4D) and HeLa (Fig. 4E) cells, where 20μM peptide induced ~50% MTT reduction. On the other hand, 10μM Aβ found to be the extreme condition rather than dose dependent effects in MG63 cell line, where the peptide cause 70% reduction of MTT (Fig. 4F). The MTT reduction induced by oligomeric peptide, however, was not suppressed by inclusion of caspase inhibitor in any tested cell lines (Fig. 4D-F), suggesting that Aβ42 induced caspase-3 like activity did not cause the cell death. The observation was consistent with previous report [66] and indicated that AB42 induced cell death might involved caspase independent pathway.

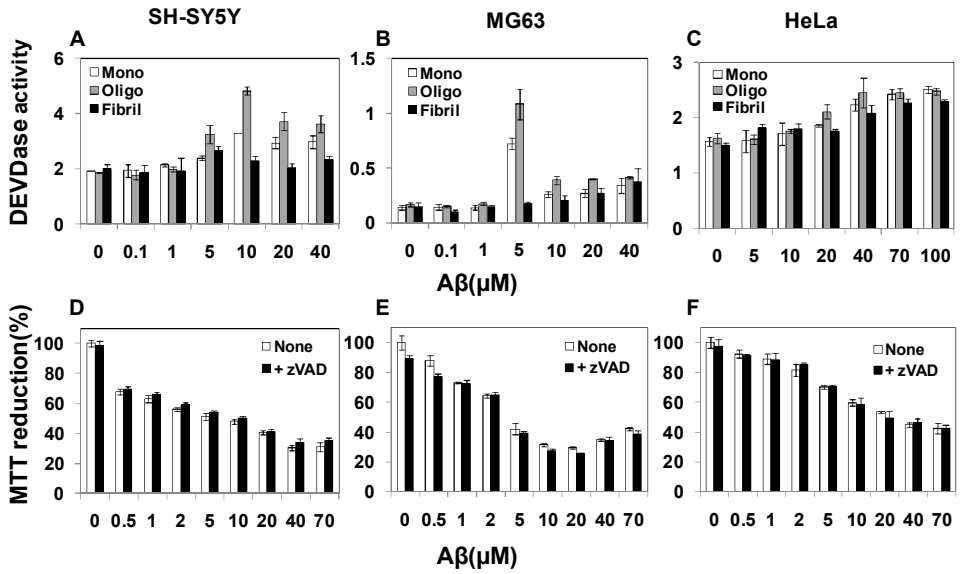

Fig. 4. Aβ42 induced DEVDase activity and cell death. (A-C) Cells were treated with monomerized, oligomerized and fibrillar Aβ42 at the indicated concentrations for 24 h. DEVDase activities were measured. **(D-F)** Cells were treated with oligomerized Aβ42 for 24h at indicated concentration in the absence or presence of z-VAD-fmk at 20 μM. Then, the survival rates were accessed by MTT reduction assay. The results are the mean ± S.D. of three independent experiments.

III-1-2. Aβ42 suppresses activation of DEVDase

Although the activation of DEVDase (mainly activity of caspase-3) was consistently detected in various types of cells treated with Aβ42, the activation was often limited (2~3-fold of healthy cells) (Fig. 4A-C). The result suggested the possibility that differential activation might be due to a negative effect of Aβ42 on the activation under a certain condition. To test the hypothesis, cells were treated with staurosporine (STS), a protein kinase inhibitor, concurrently with Aβ42 and DVEDase activity was measured. The concurrent treatment of STS and Aβ42 to human epithelial HeLa cells resulted in less activities of DEVDase than STS alone did (Fig. 5A), implying that Aβ42 could be inhibitory on the activation as hypothesized. The inhibitory effect was also obvious in human osteosarcoma MG63 cells (Fig. 5B). Oligomeric forms of Aβ42 at 40 μM suppressed the activation by ~80% in the both cell lines (Fig. 5 A and B). The monomerized peptide was also effective on the suppression to a less extent (Fig. 5 A and B), while the fibrillar form rarely showed the effect (data not shown). On the other hand, the inhibitory effect was relatively weak in neuroblastoma SHSY5Y cells (<50% at >70 μM of Aβ42) (Fig. 5C), implying that the inhibition could be cell-type specific.

The inhibitory effect depends on the preincubation time with Aβ42. The highest magnitude of inhibition was observed when the cells were preincubated for more than 2 h with high concentrations (>40 μM) of the peptide (Fig. 5D). Twenty μM of Aβ42 inhibited ~50% of the activity and nearly 80% suppression was observed with 40 μM of the peptide (Fig. 5D). The suppression level was maintained in a similar extent up to 8 h preincubation. It is noted that Aβ40 was

not effective in the suppression (data not shown).

Cell death induced by STS, assessed by MTT reduction assay, was suppressed by a pan-caspase inhibitor, z-VAD-fmk (Fig. 5E). It was also inhibited by Aβ42 in a dose-dependent manner (Fig. 5E). Forty μM of the peptide suppressed the cell death as effectively as z-VAD-fmk did (Fig. 5E), consistent with the inhibitory effect of the peptide on caspase activation. The assay often leads to the false decreasing results, due to the exocytosis of MTT formazon by Aβ42 peptide [116], but the results in the current study are irrelevant to it because the MTT reduction increased.

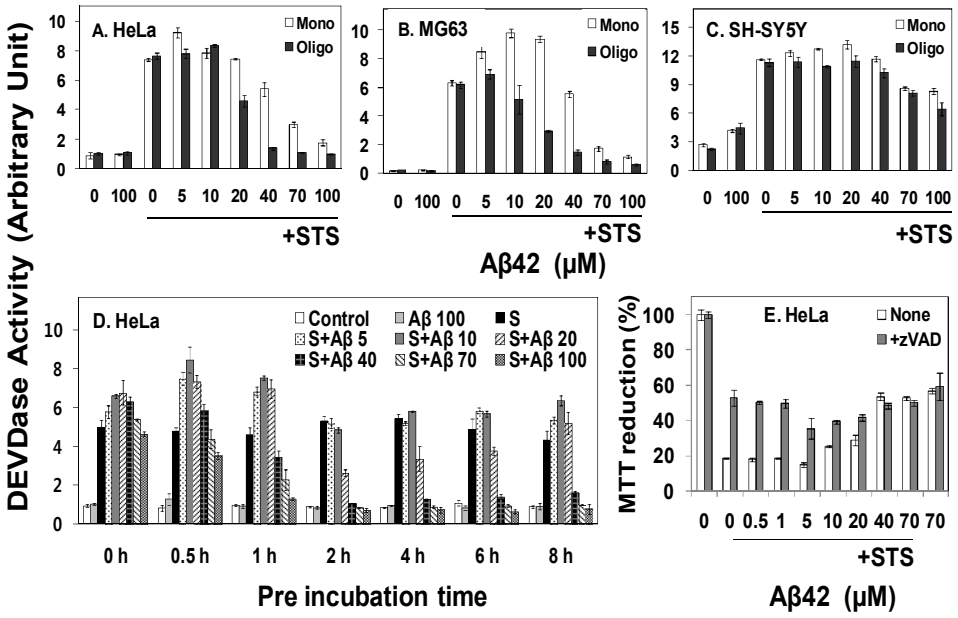

Fig. 5. Inhibitory effects of Aβ42 on DEVDase activity and cell death induced by STS. (A-C) Cells were treated with mono- or oligomerized Aβ42 at the indicated concentrations for 6 h and further incubated for 6 h with or without 0.5 μM STS. Then, DEVDase activities in the extract prepared from each cell were measured. **(D)** After treatment of HeLa cells with oligomerized Aβ42 for the indicated time, cells were further incubated for 6 h with 0.5 μM STS. Then, DEVDase activities were measured. Control was cells incubated without Aβ42 or STS. S and the numbers indicate STS and the Aβ42 concentrations in μM, respectively. **(E)** After cells were pretreated with oligomerized Aβ42 at the indicated concentrations for 6 h in the absence or presence of z-VAD-fmk at 20 μM, STS was added at 0.5 μM and incubated for additional 6 h. Then, the survival rates were accessed by MTT reduction assay. The results are the mean ± S.D. of at least three independent experiments

III-1-3. Aβ42 suppresses apoptosome formation

To identify step(s) of the apoptotic pathway induced by STS that was affected by Aβ42, the release of cytochrome c and processing of caspases and their substrate proteins were examined using the oligomerized peptide which showed higher inhibitory effect (see Fig. 5A). In the following experiments, HeLa cells were used unless indicated, because the inhibitory effect of Aβ42 was prominently observed in the cells. STS has been known to result in mitochondria-mediated apoptosis [117], which is characterized by cytochrome c release from the mitochondria, the Apaf-1 apoptosome formation, and activation caspase-9 and -3 [61]. Aβ42 alone at up to 70 μM rarely caused release of cytochrome c in the cells at the time periods (4 and 6 h), whereas the protein was invariably released upon STS treatment (Fig. 6A). The release was not affected by the inclusion of Aβ42 during the incubation, but the processing of caspase -9, -3, -8 and their substrate proteins such as DFF45/35 and Bid were suppressed by the peptide (Fig. 6B-G). The cleavage of caspase-8 induced by STS was also suppressed (Fig. 6E) whose pattern was in well accordance with those of caspases-3 and -9 (Fig. 6B and C). It is possible that an influence of Aβ42 on receptor-mediated pathway might be responsible for the suppression, but in mitochondria-mediated apoptotic pathway induced by STS, active caspase-3 was proposed to play a role in the processing of caspase-8 as a part of the amplification loop [118]. Considering this, it can be suggested that the suppressive effect of Aβ42 on DEVDase induced by STS was due to the effect on the mitochondrial pathway rather than receptor-mediated pathway.

From the results of Fig. 6A-G, it was clear that Aβ42 negatively affected the step between the release of cytochrome c and the processing of caspase-9. Thus, the next experiment was conducted to examine the effect of Aβ42 on the apoptosome formation using size exclusion chromatography. A significant amount of Apaf-1 and caspase-9 were detected at ~700 kDa in the cell extract from STS-treated cells, indicating the formation of apoptosome (Fig. 6I). The formation of apoptosome was not detected in cells treated with 20 μM Aβ42 (Fig. 6J) and it was comparable with that of non treated cells (Fig. 6H). In the cells treated with STS and 20 μM Aβ42, Apaf-1 was detected in the early fractions as in cells treated with STS alone, but caspase-9, partially processed, was recovered only in the late fractions as in the non-treated control cells (Fig. 6K). In the cells treated in the same way but with 40 μM Aβ42, neither Apaf-1 nor caspase-9 were detected in the early fractions (Fig. 6L), clearly indicating the suppressive effect of Aβ42 on the formation of the Apaf-1 apoptosome protein complex.

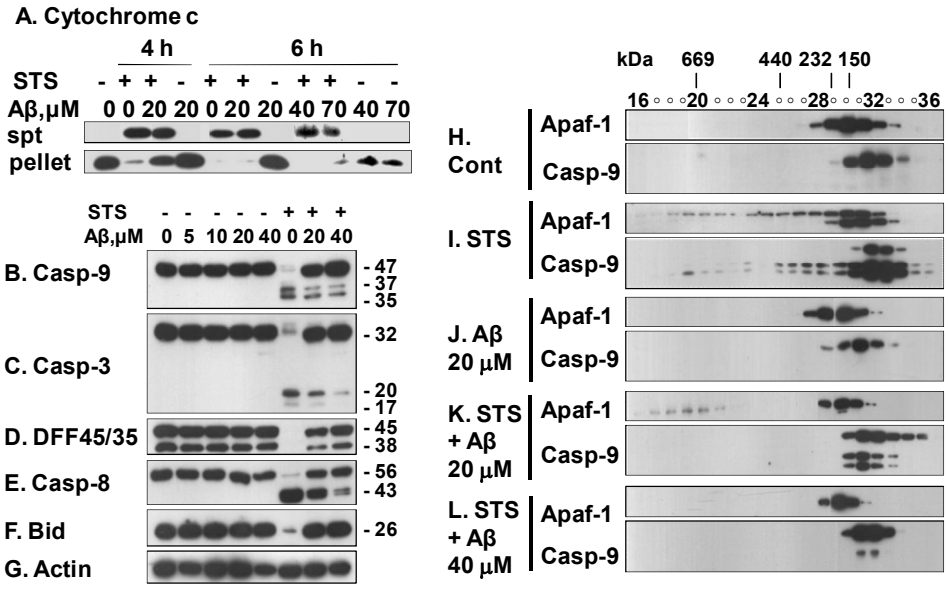

Fig. 6. Effect of Aβ42 on cytochrome c release, processing of caspases, DFF, Bid and the formation of Apaf-1 apoptosome. (**A-G)** After HeLa cells ($1.6x10^6$) were incubated in the absence or presence of oligomerized Aβ42 at the indicated concentrations for 6 h and further incubated for 4 or 6 h with Aβ42 at the same concentration and 0.5 μM STS, cytochrome c release, the processing of caspases (casp), DFF45 and Bid were assessed by immunoblot analysis. Spt and pellet in cytochrome c indicate soluble and precipitated parts of the cell extracts, respectively. Actin was employed as a loading control. The relative molecular weights (in kDa) were indicated at the left. Data are a representative of at least three independent experiments. **(H-L)** HeLa cells ($1.6x10^6$) were preincubated without (Cont, STS) or with (STS+Aβ and Aβ) oligomerized Aβ42 for 6 h and further incubated in the absence (Cont and Aβ) or presence (STS and STS+Aβ) of 0.5 μM STS for 6 h. The extract prepared from the cells (1~1.5 mg) was fractionated by gel filtration chromatography as described previously [109]. The fractions were analyzed by immunobloting for Apaf-1 and caspase-9. The standard molecular markers are indicated above the scale with elution fractions.

III-1-4. Extract prepared from Aβ42-treated cells is less active in formation of apoptosome

In an attempt to probe the mechanism of the inhibitory effect of Aβ42 on the formation of apoptosome, the extract prepared from cells treated with the peptide was analyzed and compared with that of non treated cells. Addition of 1 mM dATP and cytochrome c at varying concentrations to the extract prepared from healthy cells (HCE) induced the activation of DEVDase activity in a cytochrome c dose-dependent manner (Fig. 7A). The lower magnitude of activation was detected in the extract prepared from Aβ42-treated cells (ACE) (Fig. 7A). Consistently, the less processing of caspase-3 was observed in ACE than in HCE, which may be due to the less activation or/and activity of caspase-9 in the ACE (Fig. 7B). Parts of Apaf-1 and none of caspase-9 were detected in the early fractions (fr. 13-25) in the size exclusion chromatography of ACE incubated with dATP and cytochrome c, indicating that the formation of apoptosome was less in the cell extract compared with HCE (Fig. 7C). It is noted that Aβ42 was eluted at the several different fractions (Fig. 7C). Meanwhile, the activation of DEVDase by purified caspase-9 was comparable in the both cell extracts (Fig. 7D). Furthermore, the activation of DEVDase by dATP and cytochrome c in HCE was inhibited by directly added Aβ42 in a dose-dependent manner, while the activity was not affected once activated (Fig. 7E control), implying that Aβ42 directly affected the activation of caspase-9. Analysis with Aβ40 or the cell extract prepared from SHSY5Y cells, tested for the comparison, also showed the comparable results (Fig. 7E). All these data together indicate that ACE is less active in the formation of apoptosome and activation of caspase-9.

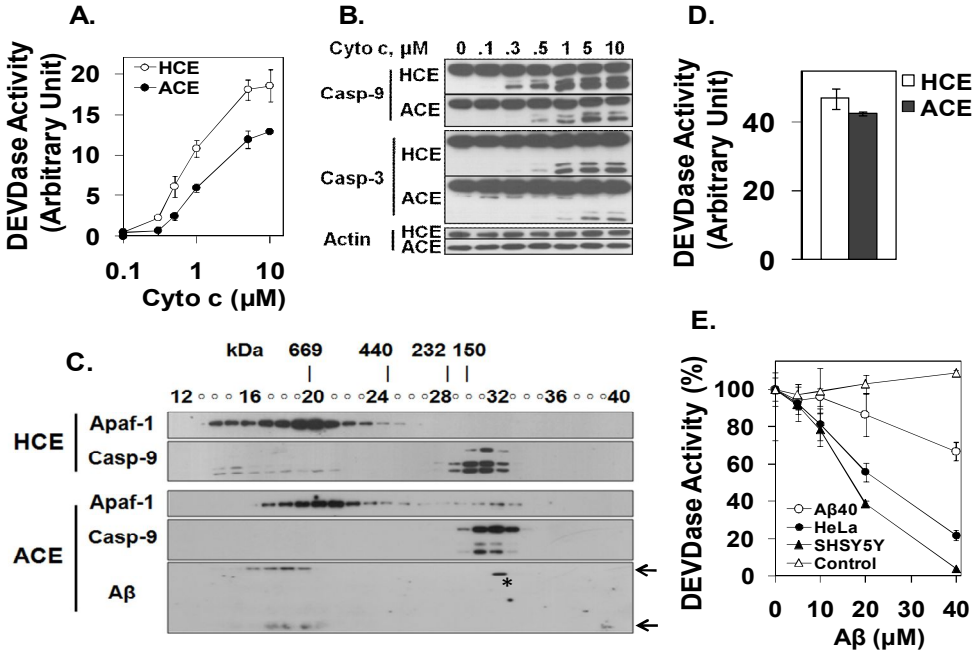

Fig. 7. Analysis of the Aβ42-treated cell extract. (A-C) *In vitro* apoptosis was induced by addition of 1 mM dATP and cytochrome c at the indicated concentration (**A and B**) or 1 μM (**C**) to the extracts (100 μg for **A**, **B** and 900 μg for **C**), prepared from healthy (HCE) or Aβ42 (20 μM)-treated (ACE) HeLa cells. The cell extracts were incubated for 1 h and assayed for DEVDase activity with 10 μM ac-DEVD-AMC (**A**), processing caspase-3 and -9 (**B**), and formation of apoptosome as described in Fig. 3 (**C**). The arrows indicate oligomer (upper) or monomeric(lower) Aβ42. The star indicates Aβ42 that might be from caspase-9 bound form. **(D)** HCE or ACE (100 μg) was incubated with purified caspase-9 (1 μg) for 1 h and assayed for DEVDase activity as in A. **(E)** *In vitro* apoptosis was induced by addition of 1 mM dATP and 1 μM cytochrome c to the extracts (100 μg) prepared from healthy HeLa (○, ●, Δ) or SHSY5Y (▲) cells for 1 h in the absence (Δ) or presence of Aβ42 (●, ▲) or 40 (○) at the indicated concentrations and then, assayed for DEVDase activity with 10 μM ac-DEVD-AMC. DEVDase activity for control (Δ) was measured in the presence of Aβ42 at the indicated concentrations. The results of A, D and E are the mean ± S.D. of three independent experiments.

III-1-5. Binding of caspase-9 to Aβ and formation of inclusion body

Previously, it has been reported that the formation of apoptosome could be suppressed by the physiological concentration of potassium [109]. The current results of the cell-free experiments, however, imply that ability of the apoptosome formation was abated in ACE, which might be due to interaction of Aβ42 with component(s) of the apoptosome. The possibility was examined by immunoprecipitation study. Several proteins of apoptosome including Apaf-1 have been pool down using antibody specific for each protein. Aβ42 was found to coimmunoprecipitate only with caspase-9 (Fig. 8A). Similarly, the coimmunoprecipitation of caspase-9 with the peptide was detected in the extract prepared from the cells treated with Aβ42 and STS (Fig. 8A), further supporting entrance of the peptide into cells and negative roles of the peptide in the formation of apoptosome by binding to the protein. The immunocytochemistry image of the cells that were probed with anti-caspase-9 and anti-Aβ antibodies were found overlapped, consistent with the colocalization of the two proteins (Fig. 8B). The colocalization of caspase-9 and Aβ in brain tissue from Tg2576 was also observed in the similar experiments (Fig. 8C). Indeed, in some cells, caspase-9 found to form inclusion body like structures (Fig. 8B, Aβ lanes), suggesting that binding might leads to the formation caspase-9:Aβ protein complex and finally sequestration of caspase-9. Similar inclusion body like structure was also found in cells treated with Aβ42 and STS (Fig. 8B, Aβ+STS lane) and in brain tissue from Tg2576 (Fig. 8C).

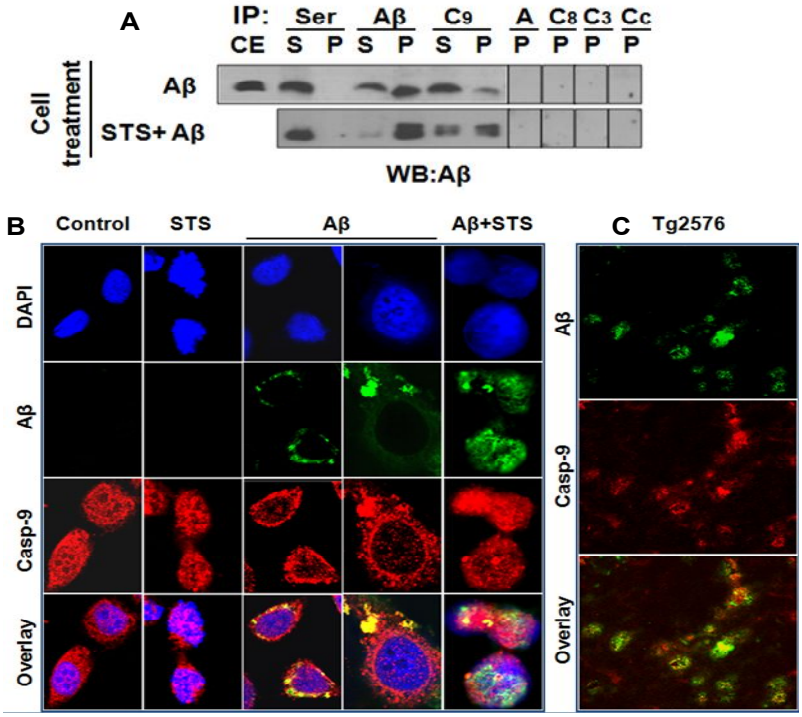

Fig. 8. Aβ42 interacts with caspase-9 and form inclusion body. (A) Immunoprecipitation analysis of the cell extracts prepared from Aβ42 (20 μM)-treated HeLa cells ($1.6x10^6$). Supernatants were obtained by centrifuge and subjected to immunoblot analysis. Ser indicate the serum contacting anti-mouse immunoglobulin which was added as a negative control. C9, A, C8, C3, and Cc indicate caspase-9, Apaf-1, caspase-8, caspase-3 and cytochrome c, respectively. The result is one representative of at least three equivalent experiments. **(B and C)** Procaspase-9 and Aβ colocalized in HeLa cells (**B**) and Tg2576 mouse brain tissues (**C**). Primary mouse anti-Aβ (6E10) and rabbit anti-caspase-9 (p10) antibodies in addition to secondary anti-mouse IgG–FITC and anti-rabbit IgG-Rhodamine antibodies, were used to detect intracellular Aβ (green) and caspase-9(red), respectively. Nuclei were seen with the nucleic acid fluorochrome DAPI (blue). Images were visualized using a confocal microscope (LSM510, Carl Zeiss).

III-1-6. CARD domain is important for the binding of procaspase-9 to Aβ42

The interaction of caspase-9 and Aβ42 was further examined using purified proteins. A large portion of procaspase-9 protein was recovered in the earlier fractions (13-25) in the size-exclusion chromatography when the protein was incubated with 20 μM Aβ42 for 1 h before the chromatography, implying its strong interaction with Aβ42 (Fig. 9A).On the other hand, much less (processed) caspase-9 proteins were eluted in the earlier fractions in the same chromatography when incubated in the same way, while no protein was detected in the case of caspase-9 lacking the CARD domain (ΔCARD) in the fractions (Fig. 9A). Measured K_D value of procaspase-9 for Aβ42 was ~0.8 μM, while that of processed caspase-9 was more than 100 μM. The results indicated that CARD domain and processing appear to be important for the binding.

Next, the effects of the peptide on the activity of purified proteins were assessed. Enzymatic activity of procaspase-9 was inhibited by Aβ42 (Fig. 9B), while the activity of processed caspase-9 was barely inhibited by Aβ42 at the initial incubation time, but later it was in a dose-dependent manner (Fig. 9C), reminiscent of typical slow binding inhibition [119]. While, ΔCARD was not inhibited by Aβ42 (Fig. 9D). Interestingly, caspase-9 activity in partially purified apoptosome was neither suppressed by the peptide (Fig. 9E), implying that once the protein complex is formed, caspase-9 activity is resistant to Aβ42 inhibition.

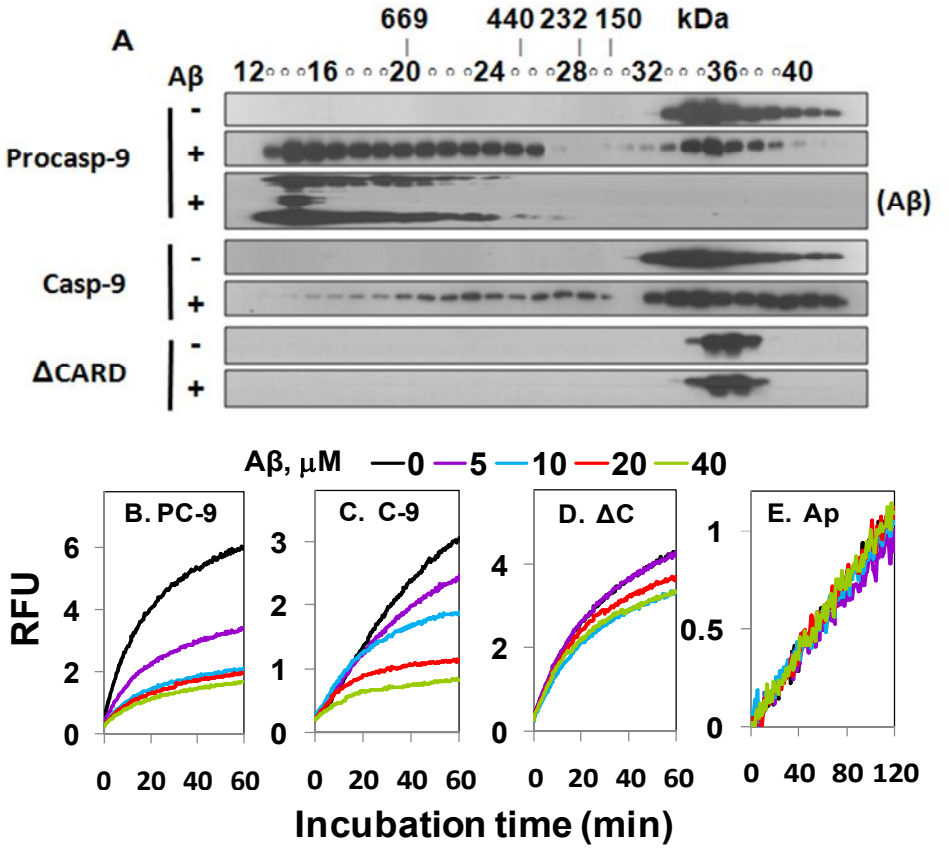

Fig. 9. Binding of Aβ42 with purified proteins and its effects on enzymatic activity. (A) Ten μg of purified procaspase-9 (E306A/D315A/D330A triple mutant), caspase-9 and ΔCARD-caspase-9 were incubated with or without 20 μM Aβ42 for 1 h and subjected to gel filtration chromatography as described above. The fractions were analyzed by immunoblot analysis for caspase-9 and Aβ(indicated at right). The standard molecular markers are indicated above the scale with elution fractions. **(B-E)** Each caspase-9 (1 μg) or apoptosome (40 μl of 1.5 ml pooled fractions) partially purified from the cell extract (2 mg) treated with 1 mM dATP and 1 μM cytochrome c using the size exclusion chromatography was incubated with Aβ42 at the indicated concentrations and their activities were assayed using 50 μM LEHD-AMC as a substrate.

According to the Aβ hypothesis, the peptide plays a central role in Alzheimer's disease (AD). Aβ has various functions: for example, it binds to receptors [31,32,33,34,37], interacts with intracellular proteins [47,48,50,51] and forms a channel-like structure on the plasma membrane[40,41]. The eventual consequence of those intra- and extracellular interaction is the induction of cell death by the peptide. The activation of caspases has been extensively reported in the death process [57,64,66]. For this reason Aβ is considered as a pro-apoptotic agent. The present study, however, identified new interaction of Aβ to a caspase family protein and demonstrated that the peptide can inhibit the activation of caspase and apoptosis.

The data of the present study indicate that Aβ42 directly interacts with procaspase-9, which causes the suppression of the mitochondria-mediated apoptosis. This may provide a molecular explanation for the relatively lower activity of caspase in cells treated by the peptide (Fig. 4A and B). The activation of caspase has been an important indicator of Aβ cytotoxicity and the apoptotic pathway is a potential target for the therapeutic control of AD [120], but based on the findings of the present study, it strongly indicate that caspase activation assay is an unreliable indicator of Aβ-mediated cell death. Furthermore, these findings suggest that previous results on apoptotic properties of Aβ peptide [64,65,66] should be interpreted with caution if apoptosis was inferred using caspase activation. The present study, however, proposed a new interaction mechanism of Aβ peptide with an intracellular protein and its eventual consequences on cell death, which shown in Fig. 10. The final corollary of the interaction was the formation of procaspase-9 inclusion body, which effects to the cell remain to be elucidated by further study.

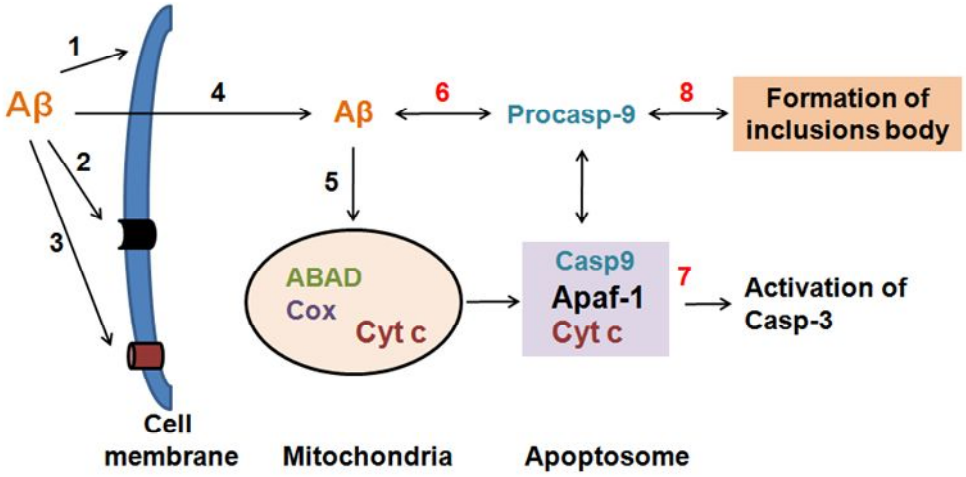

Fig. 10. Summary of proposed model for effect of Aβ on cells death. The cytotoxic effect of Aβ42 could be through the peptide's direct interaction with cell membrane (1), binding to a specific receptor (2), forming a channel-like structure on cell membrane (3), interaction with unknown intracellular targets (4), and interaction with mitochondrial proteins such as ABAD or cytochrome c oxidase (5). The current study demonstrates the interaction of the peptide with procaspase-9 **(6)** and as results, formation of the Apaf-1 and activation of caspase- 9 and -3 are suppressed **(7)**. Procaspase-9 forms the inclusion body as a result of the interaction with Aβ42 **(8)**.

The apoptotic pathway is a potential target for the therapeutic control of AD, but the current data evoke reconsideration of the action. The present study showed that Aβ interact with a crucial apoptotic protein and consequently formed protein inclusion. In a short period of time the peptide negatively affects a cell death pathway, as shown in the current study, but eventually, should cause damage to cells like misfolded proteins accumulated in many neurodegenerative disorders including Hungtington's and prion disease.

III-2. Extracellular protein, MBP, interfere Aβ aggregation and accumulates non toxic oligomers

III-2-1. MBP inhibit fibrilogenesis of Aβ42

The toxicity of Aβ peptides involves its self assembly from monomers to β-sheet rich fibrils. During the assembly process several soluble intermediate of oligomers and protofibrils are derives which found to be the most toxic components. Several chaperones have been found profoundly regulate the Aβ assembly and toxicity. To investigate the effect of an extracellular protein, MBP, on Aβ aggregation and cytotoxicity, initially the capability of this protein to inhibit process of fibrilogenesis was examined. Since chaperones to Aβ ratio have been reported an important factor to exert the inhibitory properties, different amounts of MBP were taken in the experiment with 20μM of Aβ42 and incubated for 12h. The amounts of fibrilar Aβ in the reaction mixtures were measured by well known Th-T assay.

As shown in Fig. 11, MBP decreased the amount of fibrilar Aβ in reaction mixture dose dependently and it completely inhibited the fibrilogenesis process at as lower as ~0.015 molar ratio, where the amount of fibril in reaction mixture was comparable to without incubated Aβ sample. The lowest MBP/Aβ ratio, 0.005, was unable to protect the process, while increasing the ratio to 0.01 decreased the fibril amount ~30%. The fluorescence also measured for the highest concentration of MBP (0.8μM) without Aβ to exclude the possibility of Th-T and MBP interaction. The results indicated that Aβ self assembly was inhibited in presence of MBP.

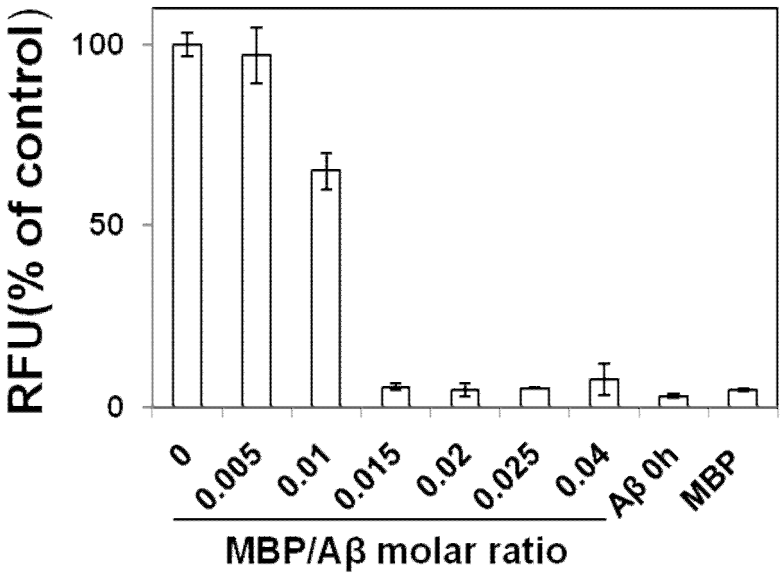

Fig. 11. Inhibition of Aβ42 fibril formation by MBP. After incubation of Aβ42 in absence or presence of indicated ratios of MBP to Aβ for 12 h at 37^{o}C in PBS, reaction mixtures (not centrifuged) were subjected to thioflavin T binding assay. Aβ 0h represents the fresh peptide without incubation. RFU is relative fluorescence unit. The *error bars* indicate ± standard deviation obtained from three independent experiments.

III-2-2. MBP regulate the Aβ42 aggregation and accumulate oligomeric species

It has been reported that chaperone interact with Aβ and accumulate oligomers [77]. To investigate whether the inhibition of fibrilogenesis in presence of MBP accumulates oligomeric forms of Aβ, 20μM of Aβ42 were incubated in presence of different amounts of MBP for 6h, 12h and 24h, and the reaction mixtures were then examined by well characterized SDS-PAGE and western blotting.

A considerable amount of oligomers were visible at the ratios from 0.01 to 0.02(Fig. 12A-C). Significant amount of small oligomers of <20 kDa, provably trimers and tretramers, were observed at higher ratios which become more prominent after longer incubation (Fig. 12C). The large oligomers of ~44 to ~ 100kDa were found higher amount at lower ratio (~0.01) at earlier time point (Fig. 12A), while longer incubation overwhelmingly increased the amount of large oligomers at higher molar ratios of MBP to Aβ (Fig. 12B and C). In 0.02 ratio, both small and large oligomeric species increased gradually due to lengthen the incubation times (Fig. 12A-C, right lane).

To exclude the possibility of oligomer formation, dissociation or degradation in presence of SDS and boiling [121], a chemical crosslinker was used in the parallel experiments to crosslink the accumulated Aβ species prior to analysis by SDS-PAGE. At the lowest ratio (~0.005), in comparable to Aβ alone, no differences observed in structural modulation even after 6h of incubation (Fig. 12D), while abundant of monomers were present at 0.01 ratio which completely disappeared after longer incubation (Fig. 12E-F). A clear correlation was

observed between the disappearance of both monomeric and oligomeric species and the incubation time for the ratio 0.015(Fig. 12D-F). Interestingly, some oligomers (most probably trimers, pentamers and hexamers) appeared after 12h incubation at higher ratios (0.015 and 0.02) which was visible ~ 20kDa areas (Fig. 12E-F). All of these species disappeared at 0.015 ratio after 24h, while the ratio ~0.02 was enriched most of these species along with monomers and large oligomers (Fig. 12F). The results indicated that in presence of higher amount of MBP Aβ assembly process hampered and several oligomeric intermediates accumulated.

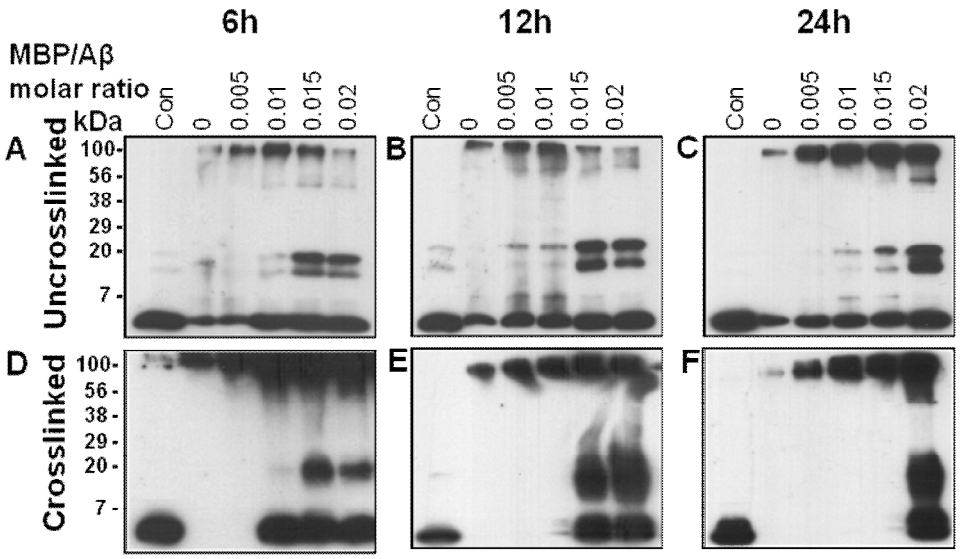

Fig. 12. **MBP accumulates the oligomeric Aβ42**. Fresh Aβ42 (20 μM) was incubated in PBS at 37 °C for 6, 12 or 24 h, either alone or in the presence of MBP at the indicated molar ratios to Aβ42. After the incubations, the peptide in the reactions was left uncrosslinked **(A-C)** or crosslinked **(E-F)** with 0.01% glutaraldehyde before being subjected to 16% SDS-PAGE and the following immunoblotting with anti-Aβ antibody 6E10. Two μl of reaction mixture was loaded for the SDS-PAGE. Con indicates a fresh Aβ42 (no incubation) each case. The numbers on the left indicate the relative molecular weights of protein markers.

III-2-3. TEM analysis of accumulated Aβ42 intermediate species

To examine the morphological structure of accumulated Aβ species, TEM study was performed in absence or presence of 0.2, 0.3 and 0.4μM of MBP. When Aβ incubated in absence of MBP for 6h (Fig. 13A) all showed clear fibrilar morphology which became large bundles of mature fibrils after 24h incubation (Fig. 13E). In presence of 0.2 μM MBP which give 0.01 ratio to 20μM Aβ , several heterogeneous species of ~3 to 10nm and predominant longer elongated structures were visualized (Fig. 13B) which after longer incubation converted to >100nm structural species, most probably the large protofibrilar intermediates or immature fibrils(Fig. 13F). While, at 0.015 ratio (MBP 0.3 μM) mostly round smaller granular structure of ~3 to 10nm along with some elongated morphology were observed at 6h time point (Fig. 13C) and upon incubation structural transition of those oligomeric species were observed as elongated branched structure of ~100nm sizes(Fig. 13G). On the other hand, at 0.02 ratio (MBP 0.4 μM) smaller bead like structures of less than 3nm to 10nm were enriched after 6h incubation (Fig. 13D), which upon incubation to 24h, converted to several structural aggregates of ~10nm elongated species and branched structure of ~100nm, along with some spherical morphology (Fig. 13H). The results confirmed the western blot analysis data and indicated that several oligomeric intermediates accumulated in presence of MBP.

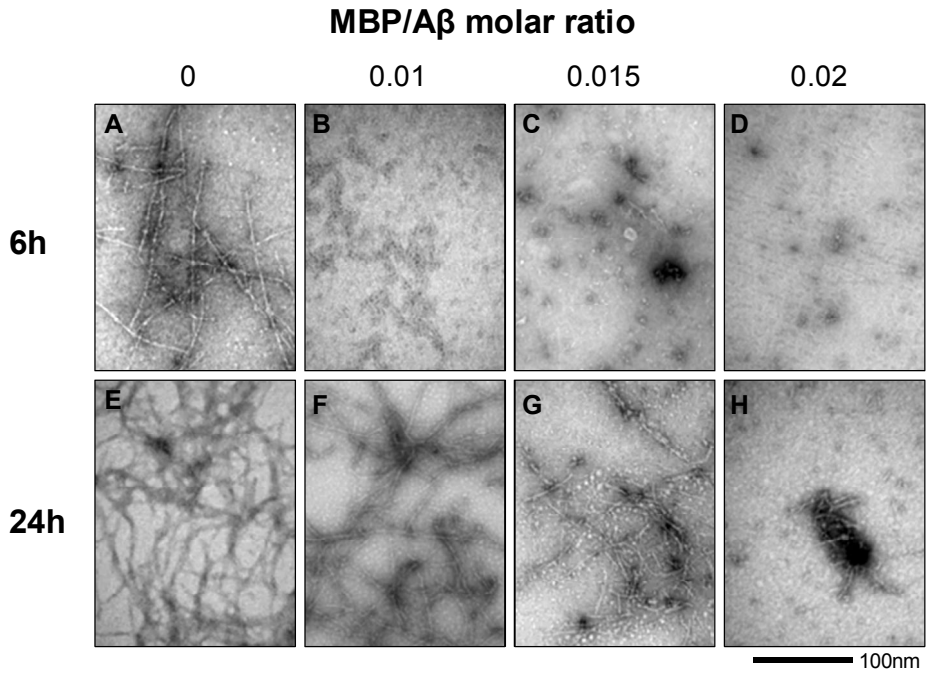

Fig. 13. TEM analysis of accumulated Aβ42 species. Aβ42 (20 μM) was incubated in PBS for 6 h **(A-D)** or 24 h **(E-H)** in the absence **(A and E)** or in the presence of MBP at the molar ratio 0.01 **(B and F)**, 0.015 **(C and G)** and 0.02 **(D and F)** to Aβ42 and then, imaged by TEM (40,000 x magnification). The *scale bars* represent 100 nm. The results are one representative of at least three independent experiments

III-2-4. MBP potentially interfere the nucleation step of fibrilogenesis

Fibrilogenesis comprises two steps; nucleation and elongation [12,13]. To investigate whether MBP inhibit the initial or later step of the assembly process, polymerization of freshly prepared Aβ42 (20μM) and extension of mature fibril seed were monitored by Th-T binding assay in presence or absence of different concentration of MBP. Freshly dissolved Aβ42 incubated at 37 ºC followed characteristic sigmoidal curve with a lag phase or nucleation phase and a growth phase or extension phase (Fig. 14A). In presence of MBP the lag phase lengthened dose dependently and even it was more than 6h for 0.3μM and ~12h for 0.4μM of MBP (Fig. 14A and C). The results indicated that MBP inhibited the formation of nucleus perhaps by interacting with smaller Aβ assemblies. Though the final equilibrium of the curve found to decrease dose dependently, interestingly, the time to reach the equilibrium level does not affected by MBP (Fig. 14A), indicating that MBP rarely affects the aggregation once nucleus is formed. The logarithmic values of fluorescence were plotted against time and linear logarithmical plots were obtained for each MBP concentration (Fig. 14B). The y intercept for the logarithomic plots of 0.4μM MBP did not coincide to those of Aβ alone or of lower concentration of MBP(Fig. 14B), which might be due to the longer lag phase for hindering the nucleation phase of Aβ assembly in presence of higher amount of MBP. *t/2* for Aβ calculated in presence of 0, 0.1, 0.2, 0.3 and 0.4 μM MPB as 1.27, 2.18, 4.06, 5.12 and 16.49 h, respectively.

To investigate the effects of MBP on elongation phase, Aβ(20μM) were

incubated with 1.1 μM preformed fibril, used as exogenous seeds, in presence or absence of several concentration of MBP(Fig. 14D). In presence of seeds, fibril elongation accelerated and proceeded to equilibrium without lag phase and reached to equilibrium within short time. Comparable to Aβ alone, the presence of MBP decreased the final equilibrium level (Fig. 14D) and slowed lower initial rate of elongation in dose dependent manner (Fig. 14F), but the time to reach the equilibrium was rarely affected by MBP, even at higher concentration of the protein (Fig. 14D). Five perfect linear logarithmical plots were obtained by plotting the fluorescence differences against times (Fig. 14E). In terms of MBP efficiency to inhibit fibril formation and fibril elongation, the presence of MBP exhibited little effects on Aβ fibril elongation than those observed on polymerization (Fig. 14 B and E). These results suggest that MBP potently inhibits the initial nucleation phase rather than affecting the elongation phase.

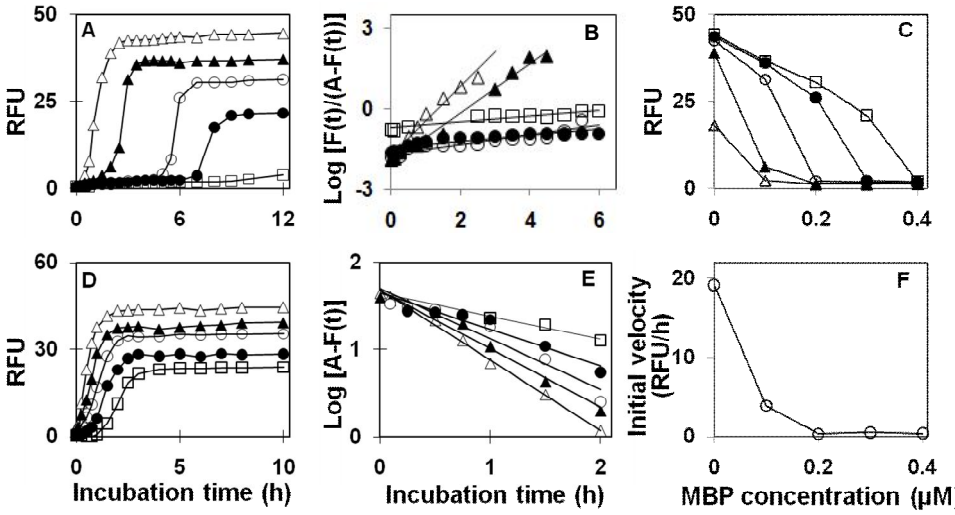

Fig. 14. Effects of MBP on Aβ42 fibrillogenesis kinetics. **(A-C)** Aβ42 polymerization assay. Fresh Aβ42 (20 μM) was incubated in PBS at 37 °C in absence (Δ) or in the presence of 0.1 μM (▲), 0.2 μM (○), 0.3 μM (●), and 0.4 μM (□) of MBP. Thioflavin T binding to the sample was measured at 490 nm at the indicated time points. RFU **(A)** and a logarithmic plot of F(t)/[A-F(t)] **(B)** against reaction time are shown. In **(C)**, RFU against concentrations of MBP was plotted for 1 (Δ), 2 (▲), 3 (○), 6 (●) and 12h (□) of the polymerization reactions. **(D-F)** Aβ42 fibril extension assay. Fresh Aβ42 (20 μM) with Aβ42 preformed fibril seed (1.1 μM) was incubated in PBS at 37 °C in absence (Δ) or in the presence of 0.1 μM (▲), 0.2 μM (○), 0.3 μM (●), and 0.4 μM (□) of MBP and the thioflavin T bindings were measured at the indicated time points. RFU **(D)** and a logarithmic plot of [A-F (t)] **(E)** against reaction time are shown. The initial velocity of fibril extension against concentration of MBP is also shown in **(F)**. The fluorescence was normalized by subtracting the value without Aβ42. A indicates F(∞).

III-2-5. MBP inhibits the secondary structural transition of Aβ42

Aβ self assembly to form fibril is accompanied by structural transition of the peptide from monomeric random coil to secondary β-sheet structure [122]. CD spectroscopy was employed to reveal effect of MBP on the structural transition of Aβ42 (20 μM). Freshly prepared Aβ(0h) adopted random coil conformation displaying negative signal at 195 nm but upon incubation for 24h it showed more negative ellipticity around 216 nm, the characteristic feature of β-sheet conformation(Fig. 15). While the co-incubation of 0.4μM MBP and Aβ42 for 24h showed no significant ellipticity ~216nm and it was comparable to that of freshly prepared Aβ, indicating the absence of β-sheet structure (Fig. 15). MBP (0.4 μM) alone showed a minor signal from 195 nm to 220 nm. The results indicated that higher concentration of MBP abolish the secondary structural transition of Aβ42.

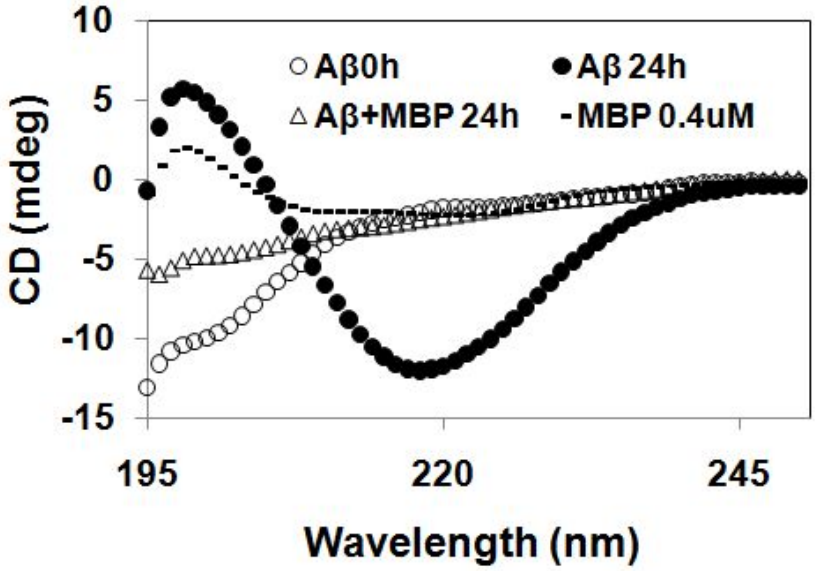

Fig. 15. CD analysis of Aβ42 structural transformation. Twenty μM Aβ42 was incubated in PBS at 37 °C for 0 h (○) and 24 h in the absence (●), or in the presence of 0.4 μM of MBP (∆) and subjected to CD analysis. In Aβ+MBP group, the values are shown after subtraction of the value demonstrated by only MBP (-) after 24h incubation. The results are one representative of at least three independent experiments

III-2-6. MBP showed protective effect against Aβ42 mediated cytotoxicity

It has been reported that oligomeric Aβ are more toxic than fribrilar species. The above results clearly showed that MBP inhibit the Aβ fibrilization preferentially at nucleation step and accumulates several oligomeric species. To examine whether the MBP accumulated oligomeric Aβ are toxic or non-toxic, cell survival have been measured in human neuroblastoma SH-SY5Y cells by MTT assay.

Aβ (20μM) alone caused ~40% cell death after 24h of treatment (Fig. 16A). Surprisingly, in presence of MBP significant cell death inhibition was observed in dose dependent manner and more than 30% cell survival enhanced at higher molar ratio (Fig. 16A, barren bar). The results were also consistent with cell viability measured in presence of pre-accumulated Aβ species by MBP (Fig. 16A, filled bar), where the oligomeric species were accumulated by co-incubation of Aβ and MBP for 12h and then exposed to cells for further 24h. The result reversely correlated with the accumulation of oligomeric species by higher MBP/ Aβ ratio (see Fig. 12 and 13), implying that MBP accumulated Aβ oligomers were non-toxic to the cells.

The effect of MBP on toxicity mediated by oligomeric Aβ also observed by treating cells with oligomeric Aβ42 [108] in absence or presence of MBP (Fig. 16B). Aβ alone induced more than 50% death within 24h, while the presence MBP inhibited dose dependently and ~20% cells were rescued at 0.02 molar ratio (Fig. 16B, barren bar). Similar level of cell viability enhancement was observed when oligomeric Aβ pre-incubated with MBP and exposed to the cells (Fig. 16B, filled bar). In comparison with Aβ monomeric form, MBP was less effective to oligomeric form to abrogate the cytotoxic effects.

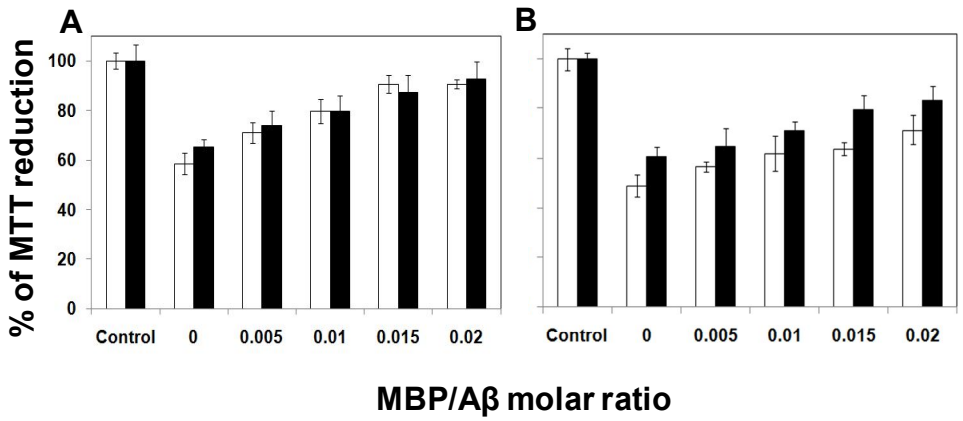

Fig. 16. Inhibition of Aβ42 cytotoxicity by MBP. A dose-dependent inhibition of Aβ42 mediated toxicity to human neuroblastoma SH-SY5Y cells has been shown. Monomeric **(A)** or oligomeric **(B)** Aβ42 (20 μM), either directly (barren bar) or after 12h pre incubation (filled bar) in absence or presence of indicated ratio of MBP to the peptide, were exposed to cell. After 24 h of the exposure cell viability was measured by MTT assay. Control represents the untreated cell groups. The *error bars* represent ± standard deviation.

Self-assembly of Aβ produces a number of distinctive structures, such as dimers, oligomers, unstructured aggregates, and characteristic amyloid fibrils. Of these structures, oligomers are believed to be the most neurotoxic species in the development of disease [23,26]. Thus, any strategies to reduce amyloid- related phenotypes must avoid the formation of toxic oligomers by inhibiting the aggregation at a stage prior to the oligomerization and accumulation of the peptides. The chaperones have been found very effective in inhibiting the aggregation and accumulating the oligomeric structures, possibly by interacting with prefibrillar assemblies [76,82]. In line with these observations, fibrilogenesis study indicated that MBP at a certain ratio to Aβ completely blocked the fibril formation (Fig.11). Circular dicroism(CD) data also supports the finding that presence of MBP inhibited the secondary β-sheet structural transformation (Fig. 15). The consequent of the inhibition, several oligomeric species were accumulated which clearly demonstrated by westernblot analysis (Fig. 12A-F). TEM data reveal the presence of several oligomeric structures at earlier time point which converted to protofibril or fibrils like structures upon longer incubation (Fig. 13A-H). Interestingly, these oligomeric and protofibrilar species were less toxic to the SH-SY5Y cells (Fig. 16A). To confirm the cytocoxicity, oligomers were accumulated by pre-incubating with MBP and exposed to cells, which also showed similar non-toxic behavior of the accumulated intermediate species (Fig. 16A, filled bar). MBP also found to inhibit oligomeric Aβ mediated toxicity (Fig. 16B) but less effectively than those mediated by monomeric forms, suggesting the better efficiency of interaction before oligomerization. From these data, however, it may conclude that, in presence of MBP, Aβ assembly pathway might be

converted to form several structural non-toxic aggregates, which may be the amorphous structural complexes. Further, the fibrilogenesis kinetics results indicated that MBP preferentially interact with the smaller assembly and effectively hinder the initial nucleation step of fibrilogenesis rather than fibril extension step (Fig. 14A-E), indicating that hindering proper assembly during nucleation might leads to the formation of non-toxic aggregates. The findings are agreement with the report on Hsp70 and Hsp90, where the chaperones also found to inhibit Aβ aggregation at early stage of self-assembly [82]. The presence of higher amount of monomeric and oligomeric species (Fig. 12 B, C, E and F) and the lengthen the lag phase (Fig. 14 A and B) at higher MBP/ Aβ ratio suggest that the higher molar access of MBP effectively hamper both phases of oligomerization process; the paranuclei (pentamer/ hexamer unit) formation and the paranuclei association [20]. The lower molar access, however, may weakly obstruct the processes.

The accumulation of several intermediate species and enhanced cytotoxic effect have been reported in presence of clusterin [80] and αβ-crystalline [84]. Lee *et al,* (2005) have been reported that sHps20 efficiently inhibit the fribril formation and toxicity at lower ratio, while the higher concentration was found less effective to prevent events. sHsp20 fused to MBP was used in the study and MBP alone have been reported to be ineffective to prevent either fibril formation or cytotoxicity. One possibility of the contrasting result might be the type of Aβ which have been found affected varyingly by different chaperones [83]. In the study, effects of MBP and sHsp20-MBP were compared using high concentration (100μM) of Aβ40, while in the present study Aβ42 was used at 20μM concentration.

In a recent study, αβ-crystalline have been reported sHsp20 like activity to abrogate Aβ40 mediated cytotoxicity as a result of inhibition of fibril formation [123]. However, other sHsps, Hsp17.7 and Hsp27, did not inhibit the toxicity of Aβ40 despite preventing its fibril formation and accumulating different morphological structures compared to the case of Hsp20 [76], implying that Hsp17.7 and Hsp27 may not prevent the formation of smaller, toxic Aβ oligomers. The evidence of the present study demonstrated the prevention of formation of smaller oligomers which might be the cause to avert the toxicity by depriving this behavior of the modulated species and then directing the self assembly pathway to form non-toxic intermediates. The SDS resistance, Th-T negative, devoid of secondary structure and non-toxic properties of the accumulated intermediates in presence of MBP strongly supports the possibility of off-pathways conformation [124].

Several sHps have been reported to inhibit Aβ toxicity without effecting aggregation, rather, by inhibiting the localization of Aβ on the cell surface [83], and thus inhibits ongoing nucleation dependent aggregation on the membrane, one mechanism by which Aβ cause toxicity [125]. In the study, Hsp20 has been reported to interact with the soluble Aβ and inhibit the aggregation whereas HspB2/B3 neither bound soluble Aβ nor affected its aggregation. In this context, data of the present study supports the interaction of MBP with smaller soluble Aβ assembly at initial phase of aggregation (Fig. 14B) rather than with large aggregates (Fig. 14E). Accordingly, the possible effects of MBP to inhibit the localization of the Aβ species to cell surface, hence to abrogate the cytotoxicity cannot be excluded. Thus, cytoprotection of MBP may not be only due to

remodeling the oligomeric species but also MBP may sequester monomeric form of Aβ to inhibit cell surface aggregation and toxicity.

Several proteins including chaperones have been found to influence Aβ assembly which, in some cases, leads to controversial results [84,87]. MBP, mostly used as fusion protein and in context of this use act as a chaperone by proper folding of fusion partner, in the present study have been found to regulates the assembly of Aβ at an earlier stage of aggregation. The consequent of the regulation was oligomeric species which found to be non-toxic to human neuroblastoma SH-SY5Y cell. The study indicate one switching mechanism of Aβ42 assembly to remodel it non-toxic aggregates which may accommodate to clarify the aggregation machinery of Aβ peptide.

III-3. A natural flavonoid, keampferol-3- rhamnoside (K-3-rh), inhibits the Aβ42 aggregation and cytotoxicity

III-3-1. K-3-rh and other related flavonoids inhibit Aβ mediated cell death

Flavonoids are suggested to be neuroprotective and multiple mechanisms of the protection have been demonstrated for this group of phenolic compounds [126]. In the present study, the cyto-protective effects of several flavonoids (Fig. 17) were examined in initial experiment and the inhibitory mechanism of a mono flavonoid, K-3-rh, against Aβ fibrilogenesis and cytotoxicity was scrutinized. Aβ42 peptide (20μM) alone was able to induce ~50% cell death when exposed to human neuroblastoma SH-SY5Y cells for 24h, while the most of flavonoids examined (20μM) rescued the cells in different extent (Fig. 18A). Keampferole-3-rhamnoside (K-3-rh), Quercitrin(Q), Keampferol-3-rutinoside(K-3-ru), Quercetin di hydrate (QdiH) and Keampferol(K) inhibited the Aβ mediated toxicity at a similar level, where K-3-rh found to be the best compound which enhanced ~30% cell survival with no toxic effect to the cells(Fig. 18A). On the other hand, Gallic acid methyl ester (GAME) and Quercetin hydrate (QH) were less effective against Aβ42 toxicity and GAME showed toxic effect to the cells when treated alone.

The dose dependent cyto-protective effects of three similar structural compounds, K-3-rh, Q and K-3-ru, further examined at several concentrations (Fig. 18B). K-3-rh inhibited the Aβ cytotoxicity dose dependently, where at 40μM ~ 40% cell survival enhancement was observed in compare to Aβ alone

(Fig. 18B). On the other hand, dose dependent cytoprotective effect of Q and K-3-ru was found till 20μM (Fig. 18B), while the higher concentration of these flavonoid found to kill cells when treated alone (data not shown). No toxic effect to the cells was found even at 50μM of K-3-rh alone (data not shown). The results indicated that K-3-rh might be potential against amyloidogenesis of Aβ peptides.

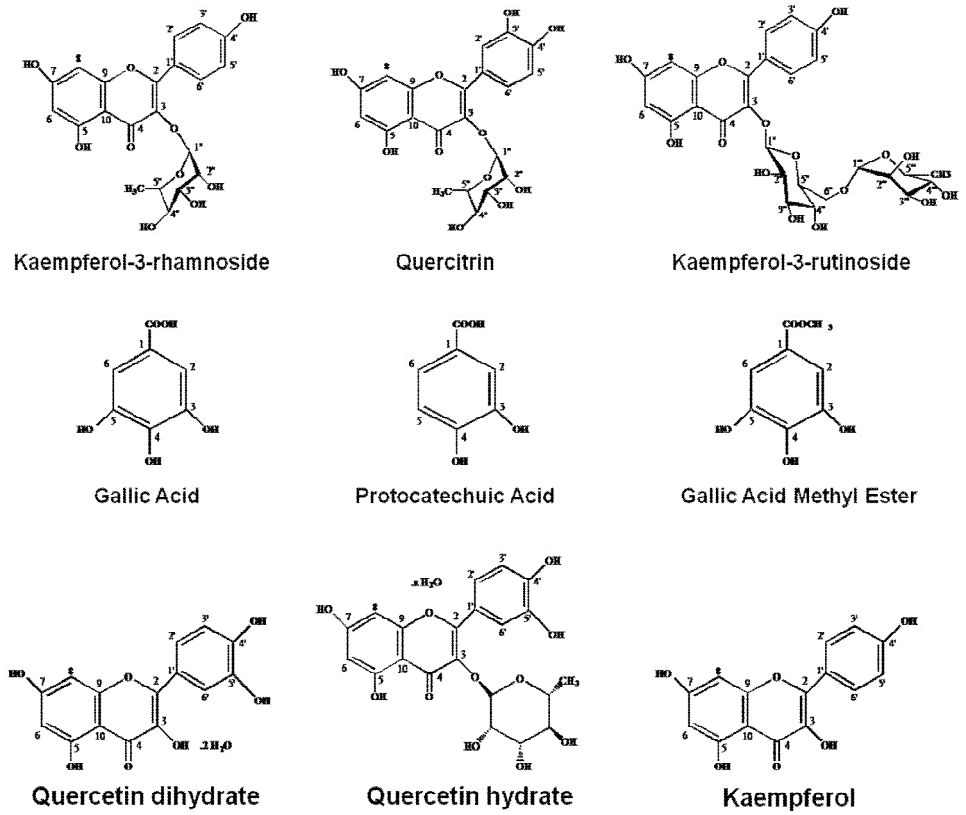

Fig. 17. Chemical structures of flavonoids with previously reported anti-amyloidogenic molecules. Structures of K-3-rh and other flavonoids are shown (structures not drawn to scale).

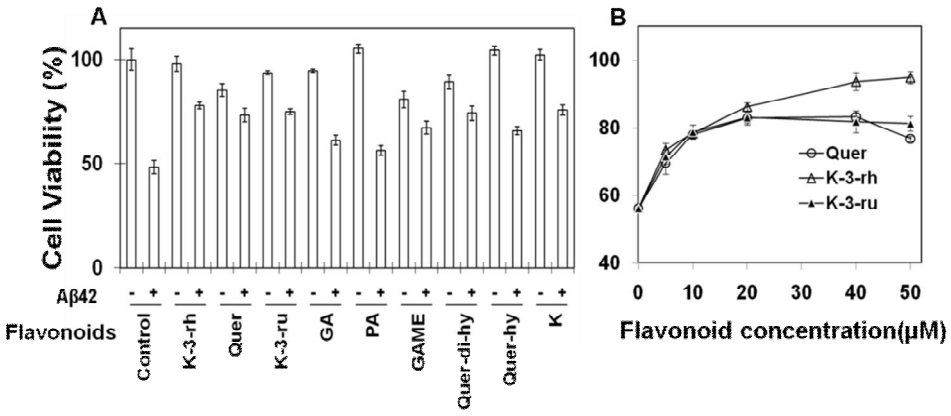

Fig. 18. Effects of flavonoids on Aβ42 induced cellular toxicity. (A) Cells were treated with/without Aβ42 (20μM) and/or indicated biflavonoids (20μM) for 12 h. **(B)** Cells were exposed to Aβ42 (20μM) in presence of 0-50μM of indicated flavonoid for 24h. Cell viability was assessed by MTT reduction assay and survival (%) was compared with untreated (control) cells.

III-3-2. K-3-rh inhibits Aβ42 polymerization and fibril extension and disintegrates mature fibrils

To examine the effect of K-3-rh on fibril formation of Aβ42, the peptide was incubated in presence of several concentrations of K-3-rh and fibrilogenesis activity was measured by Th-T assay. Aβ(20μM) alone showed characteristics sigmoidal curve when incubated at 37^{o}C (Fig. 19A). In presence of 0-40 μM K-3-rh, fibrilogenesis was inhibited dose dependently by affecting both the time to reach equilibrium and the level of the final equilibrium of the curve. Common logarithms of florescence data fitted well in logistic equation (Fig. 19D). $t/2$ for Aβ42 (20 μM) calculated 44.65, 48.26, 46.99, 38.92, 39.56 and 34.10 min, respectively, in presence of 0, 5, 10, 20, 30 and 40 μM of K-3-rh. The IC_{50} value of K-3-rh for inhibition of Aβ42 polymerization calculated as 30μM.

The fibril extension experiment were performed by incubating fresh Aβ42 (20μM) with 1.1 μM preformed Aβ42 fibril (seed), which showed the increase of fluorescence hyperbolically without lag phase (Fig.19B). The final equilibrium of the curve decreased dose dependently in presence of K-3-rh. Four perfect linear logarithmical plots with deferent y intercept were obtained by plotting logarithmic plots of fluorescence difference against times (Fig. 19E). The calculated initial velocity of fibril extension was found to be decreased in dose dependent manner when co-incubated with K-3-rh (Fig. 19F). The IC_{50} value against fibril extension found 20μM.

K-3-rh also found to be destabilized the pre formed fibril dose dependently when the mature Aβ42 fibrils were incubated with the compound (Fig. 19C).

The effectiveness of the compound to destabilize mature fibrils in terms of IC_{50} measured >40μM. The results indicated the K-3-rh effectively obstructed both nucleation and fibril extension steps of fibrilogenesis as well as it disaggregated the preformed fibrils.

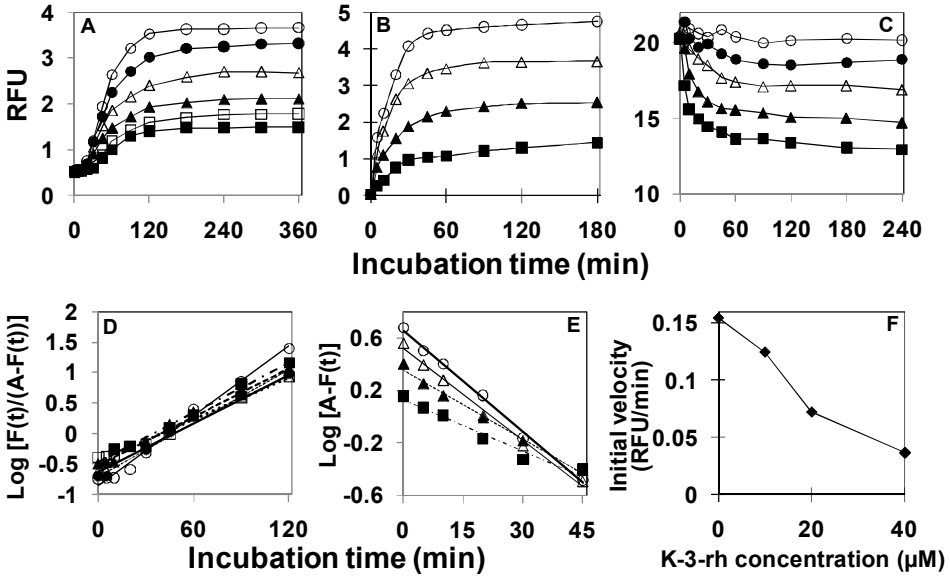

Fig. 19. K-3-rh inhibits of Aβ42 fibrillogenesis. **(A)** Inhibition of Aβ42 polymerization. Aβ42 (20 μM) was incubated in PBS at 37 °C in presence of 0 (○), 5(●), 10 (Δ), 20 (▲), 30 (□) and 40 (■) μM K-3-rh for 0-6 h. IC_{50} calculated as 30μM. **(B)** Inhibition of Aβ42 fiber extension. Fresh Aβ42 (20 μM) was added to 1.1μM preformed seed and incubated at 37 °C in presence of 0 (○), 10 (Δ), 20 (▲), and 40 (■)μM K-3-rh. IC_{50} value calculated as 20μM. **(C)** Dissolution of preformed Aβ42 fibrils in presence of 0 (○), 5(●), 10 (Δ), 20 (▲), and 40 (■) μM K-3-rh. IC_{50} found > 40μM. **(D)** Logarithmic plot of $F(t)/A-F(t)$ versus reaction time obtained from polymerization assay. **(E)** Logarithmic plot of $A-F(t)$ versus reaction time obtained from fiber extension assay. **(E)** Effect of Aβ42 concentrations on the initial rate of Aβ42 fibril extension.

III-3-3. K-3-rh inhibits the structural transition of Aβ42

Structural transition to form β-sheet structure is characteristic feature of Aβ fibrillogenesis [122]. To examine the effect of K-3-rh on secondary structural transformation, Aβ42 (20μM) was incubated with or without 20μM K-3-rh and the presence of β-sheet was detected by CD spectroscopy. As shown in Fig. 20, CD spectra of Aβ alone or with K-3-rh at 0h, demonstrated a negative absolute value at approximately ~200 nm, suggesting the presence of largely unfolded peptide at monomeric state with significant level of random coil. Upon incubation at 37^{o}C, the peptide alone exhibited the shift of a strong signal to negative ellipticity ~216 nm after 6h and the ellipticity further maximize to negative upon longer incubation, indicating the formation for β-sheet structure of the peptide[107]. The transition of random coil to β-sheet structure did not observed in presence of 20μM K-3-rh when incubated for 6h (Fig. 20). While, after 24 h incubation of Aβ with K-3-rh showed the presence of β-sheet conformation, but the amount reduced significantly which demonstrated by ~50% decrease of negative ellipticity ~217nm. The results suggest that K-3-rh does not inhibit β-sheet formation completely but it delayed the transition and significantly reduced the amount of secondary structure.

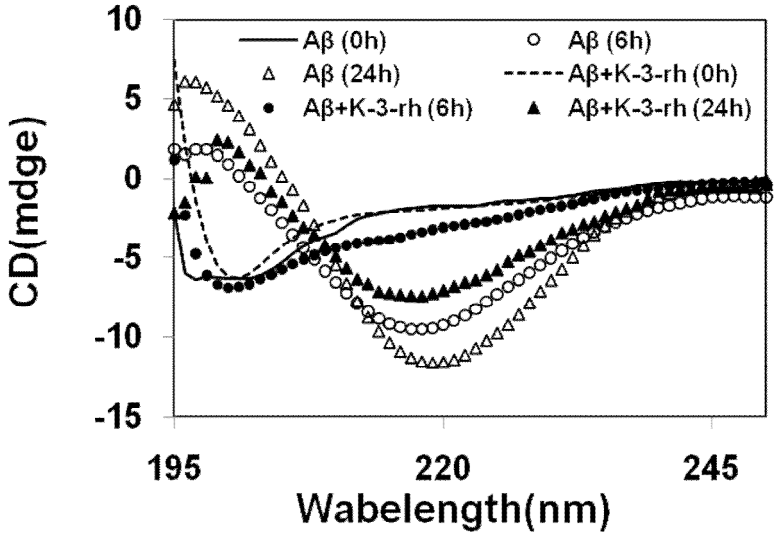

Fig. 20. K-3-rh inhibits structural transformation of Aβ42. Aβ42 (20 μM) alone or in presence of K-3-rh (20 μM) was incubated in PBS at 37 °C for 0, 6 or 24 h as indicated. Spectra were obtained by subtracting buffer background as described in materials and methods.

III-3-4. K-3-rh accumulates oligomeric species of Aβ42

Polymerization and fibril extension study showed that K-3-rh inhibits the Aβ fibril formation. Western blot analysis was performed to visualize the accumulated species as a consequent of the inhibition. Abundance of oligomeric species were observed in presence of higher concentration of K-3-rh after 6h incubation (Fig. 21A) which were visualized by two distinct bands lower than 20kD area, provably the smaller oligomers of dimric or trimeric units . Upon longer incubation, large oligomers of ~100kD were visualized along with the smaller oligomers (Fig. 21B). The predominant band below 7kD area also visualized for both shorter and longer incubation times (Fig. 21 A and B). Aggregation reaction was crosslinked to show all the possible species of Aβ that are either simply not observed in gel or susceptible to induction or degradation during separation. Monomeric Aβ disappeared after 6h even in presence of 5μM of K-3-rh (Fig. 21C). While, in presence of 10μM or more K-3-rh, a plenty of oligoligomeric species were visualized at lower than 20kD area when incubated for 6h, consistent with noncrosslink data (Fig. 21C). After 24h incubation, several structural species were observed which predominantly visualized from lower than 20kD to 100kD area. The results indicated that K-3-rh bound to oligomeric species and hinder their further polymerization. The consequent of the interaction was the formation of non toxic oligomers. The data are well accordance with the earlier report where accumulation Aβ oligomers have been found in presence of polyphenolic inhibitors[127].

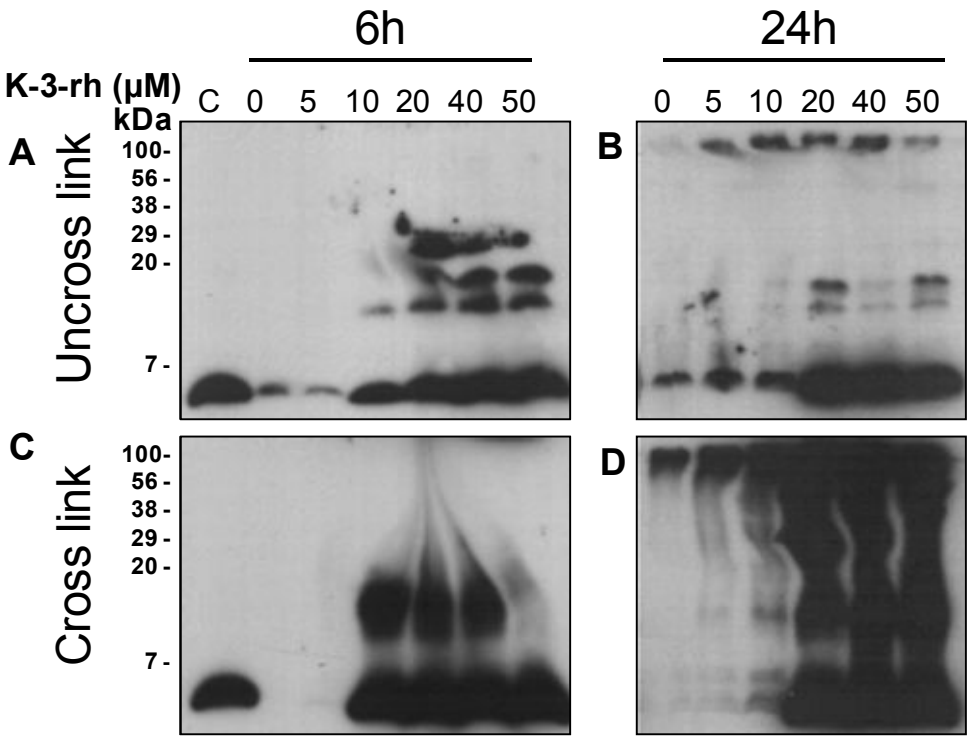

Fig. 21. Biochemical characterization of accumulated Aβ42 species. Fresh Aβ42 (20 μM) was incubated in PBS at 37 °C for 6 **(A** and **C)**, or 24 **(B** and **D)** h, either alone or in the presence of indicated concentration of K-3-rh. After the incubations, the peptide in the reactions was left uncrosslinked **(A** and **B)** or crosslinked **(C** and **D)** with 0.01% glutaraldehyde before being subjected to 16 % SDS-PAGE and the following immunoblotting with anti-Aβ antibody 6E10. Two μl of reaction mixture was loaded for the SDS-PAGE. C indicates a fresh Aβ42 (no incubation). The numbers on the left indicate the relative molecular weights of protein markers.

III-3-5. TEM observation of K-3-rh accumulated Aβ42 oligomeric species

The above results indicate that K-3-rh inhibits the fibrillogenesis and accumulates oligomeric structures. To confirm the findings, the incubated samples were imaged with TEM to visualize the accumulated species. Aβ42 (20μM) incubated alone at 37^{o}C for 12h predominantly composed of typical fibrils (Fig. 22A). In presence of K-3-rh, however, fibrilar structure was absent, instead, mostly small spherical shaped and some branched structures were observed with dose dependent effects of K-3-rh (Fig. 22 B and C). The morphology and size of these structures are consistent with those of oligomer and protofibrils previously reported [88,108,128]. The data clearly supports the presence of oligomeric species accumulated by obstructing the fibrilogenesis in Aβ samples incubated with K-3-rh.

The disaggregation of pre formed fibrils also investigated by employing TEM. fAβ42 (20μM), prepared by incubating at 37^{o}C for 3 days, showed predominantly fibrils (Fig 22 D). The fibrils were converted to smaller aggregates like shape when co-incubated with K-3-rh for 12h, where dose dependent effects were also observable (Fig. 22 E and F). It indicated that K-3-rh disintegrate fibrils and greatly alters the fibrilar shaped to smaller aggregates. The data is well agreement with our previous study where biflavonoid found similar disaggregating properties[129].

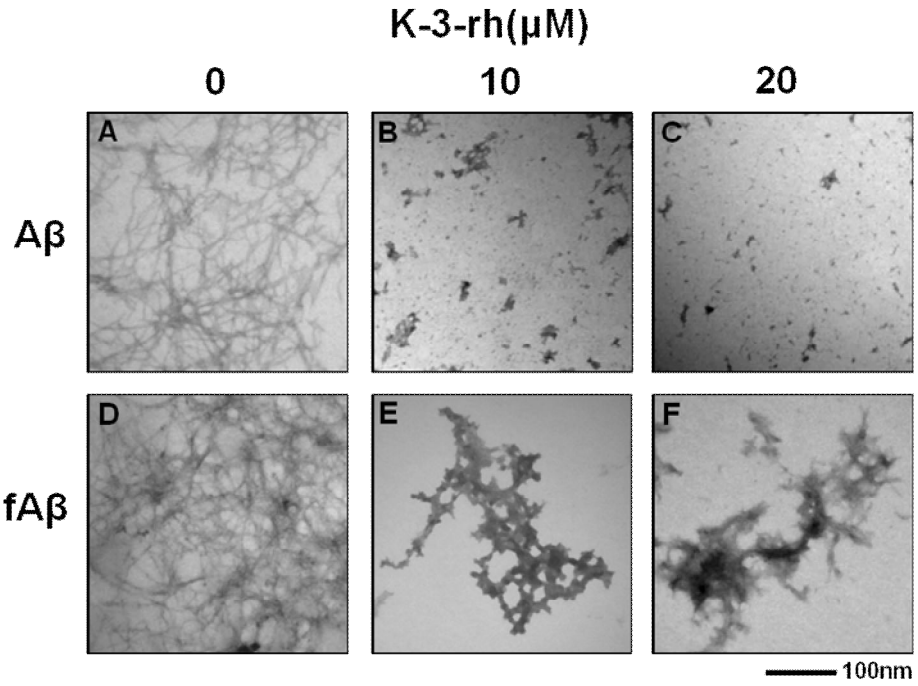

Fig. 22. TEM study of K-3-rh effects on Aβ42 fibrilogenesis and preformed fibrils. Twenty μM **f**resh Aβ42 **(A-C)** or fibrilar Aβ42(fAβ42) **(D-F)** either alone or in presence of indicated concentration of K-3-rh were incubated in PBS at 37 °C for 12 h. Aβ42 morphology was then visualized by TEM. Scale bar is shown at the bottom.

The flavonoids have been shown to abrogates Aβ aggregation, reduce cytotoxicity and oxidative stress [104,130,131]. The polyphenolic biflavonoids have been found superior to monoflavonoid in inhibiting Aβ fibrilogenesis and cytotoxicity mediated by the peptide [129]. On the other hand, in terms of IC_{50} value, some monoflavonoid have been shown only one order lower magnitude of anti-amyloidogenic properties than bioflavonoids [129,132]. In the present study, the anti-amyloidogenic and cytoprotective effects of a mono flavonoid, K-3-rh, against Aβ42 peptide was investigated to gain insights the aggregation mechanism of the peptide. The results showed that K-3-rh and other related flavonoids effectively abrogated the Aβ cytotoxicity (Fig. 18 A and B). Accumulation of oligomeric Aβ species and rescuing cells exposed to Aβ in presence of K-3-rh suggests that K-3-rh possibly neutralized the toxic effects of the peptide by hindering its self assembly. The effective inhibition of Aβ fibril extension and disintegration of preformed fibrils (Fig. 19 B and C) demonstrates that K-3-rh can interact with several structural species formed during assembly process. In presence of K-3-rh, the structural transformation of Aβ peptides delayed significantly (Fig. 20), which leads to the accumulation of several oligomeric species (Fig. 21A-D and 22B-C). The accumulated oligomeric species, however, might not be the “on pathway” or toxic oligomers since the presence of K-3-rh and other related flavonoid significantly enhance the viability of cells exposed to the peptide. The findings are well agreement with others and ours previous studies, where polyphenol (-)-epigallocatechin gallate and taiwniaflavone, respectively, found to be efficiently inhibited the fibrillogenesis of Aβ by directly binding to the unfolded polypeptides and promoted the formation of unstructured and nontoxic Aβ, resulting in off pathway, highly stable

oligomers [127,129]. The K-3-rh and other related flavonoids in the present study probably redirecting the Aβ assembly in similar way to form non toxic off pathway oligomers.

Structural composition of K-3-rh includes three phenolic groups linked with a rhamnose moiety (Fig. 18), which provides the basic structural requirements of an efficient polyphenolic inhibitor [96,132] with an extra sugar component. All flavonids with this basic polyphenolic structure in the present study (Fig. 17) found to be effective than monophenolic flavonoids to rescue cells exposed to Aβ (Fig. 18 A). K-3-rh inhibited fibril extension more effectively than nucleation (Fig. 19 D and E) and the initial rate of fibril extension decreased dose dependently in presence of K-3-rh (Fig. 19F). Further, it also disintegrated the pre formed fibrils efficiently (Fig. 19C and 22 D-F). The results suggest that K-3-rh fundamentally alters the aggregation pathway of Aβ, possibly by interacting with smaller amyloidogenic aggregates and preventing it from farther conformational change into the β-sheet. The observation is in agreement with the report that polyphenols do not interacts with the amyloidogenic monomer, instead it interact with amyloidogenic structures, and that inhibitor binding is conformation-dependent [89]. The stoichiometry of K-3-rh binding to Aβ, however, is unknown. A mechanistic approach based on structural similarities between various highly efficient polyphenol inhibitors, and relative to the well-known amyloidogenic dye Congo red has been suggested that a common efficient polyphenol inhibitors are composed of at least two phenolic rings with two to six atom linkers, and a minimum number of three OH groups on the aromatic rings [96]. These structural similarities imply for three-dimensional conformations that are essential for the non-covalent interaction with β-sheet

structures [96]. Similar speculation may be applicable for the interaction between Aβ and K-3-rh and other similar flavonoids tested in the present study.

On the other hand, K-3-rh may interacts with the aromatic residues in Aβ sequence which have been postulated the another inhibitory mechanism by polyphenolic compounds [96]. It has been suggested that the inhibitory aromatic compounds compete with the polypeptide monomers for interaction with the growing fibrils and the irreversible or improved interaction by the inhibitor result in an efficient halt of the fibrillization process [133]. Only phenolic ring by itself , however, does not efficiently inhibit amyloid formation [134] and further structural elements are necessary for the specific interaction with the amyloidogenic β-sheet conformation, creating hydrogen bonds that enhance the stability of the inhibitor–protein complex[96]. The OH groups and rhamnose structure of K-3-rh provably play that supporting role for efficient interaction with β-sheet of Aβ42 and hence abrogates its assembly.

Identifying small molecule inhibitors to inhibit Aβ aggregation and cyto-toxicity is an encouraging approach towards the therapeutic development for AD. The present study showed that a mono flavonoid with three phenolic and three OH group with a rhamnose moiety efficiently abrogates the Aβ assembly and cytotoxicity. The result confirmed requirements of the specific structural conformation for efficient inhibition of amyloidogenic assembly and interaction to β-sheet structure. The consequence of halting the assembly process, several oligomeric species derived, which showed off-pathway structural properties. The polyphenolic compounds with K-3-rh like structure, however, might be considerable to incorporate in the therapeutic strategy of AD.

IV. REFERENCES

[1] A. Goate, M.C. Chartier-Harlin, M. Mullan, J. Brown, F. Crawford, L. Fidani, L. Giuffra, A. Haynes, N. Irving, L. James, et al., Segregation of a missense mutation in the amyloid precursor protein gene with familial Alzheimer's disease, Nature 349 (1991) 704-706.

[2] D.J. Selkoe, Alzheimer's disease: genes, proteins, and therapy, Physiol Rev 81 (2001) 741-766.

[3] R.A. Armstrong, Plaques and tangles and the pathogenesis of Alzheimer's disease, Folia Neuropathol 44 (2006) 1-11.

[4] D.J. Selkoe, Alzheimer disease: mechanistic understanding predicts novel therapies, Ann Intern Med 140 (2004) 627-638.

[5] G.G. Glenner, C.W. Wong, Alzheimer's disease and Down's syndrome: sharing of a unique cerebrovascular amyloid fibril protein, Biochem Biophys Res Commun 122 (1984) 1131-1135.

[6] Y.H. Suh, F. Checler, Amyloid precursor protein, presenilins, and alpha-synuclein: molecular pathogenesis and pharmacological applications in Alzheimer's disease, Pharmacol Rev 54 (2002) 469-525.

[7] D.M. Walsh, A.M. Minogue, C. Sala Frigerio, J.V. Fadeeva, W. Wasco, D.J. Selkoe, The APP family of proteins: similarities and differences, Biochem Soc Trans 35 (2007) 416-420.

[8] J.A. Hardy, G.A. Higgins, Alzheimer's disease: the amyloid cascade hypothesis, Science 256 (1992) 184-185.

[9] J. Hardy, D.J. Selkoe, The amyloid hypothesis of Alzheimer's disease: progress and problems on the road to therapeutics, Science 297 (2002)

353-356.

[10] D.A. Kirschner, C. Abraham, D.J. Selkoe, X-ray diffraction from intraneuronal paired helical filaments and extraneuronal amyloid fibers in Alzheimer disease indicates cross-beta conformation, Proc Natl Acad Sci U S A 83 (1986) 503-507.

[11] J. Busciglio, A. Lorenzo, J. Yeh, B.A. Yankner, beta-amyloid fibrils induce tau phosphorylation and loss of microtubule binding, Neuron 14 (1995) 879-888.

[12] J.T. Jarrett, E.P. Berger, P.T. Lansbury, Jr., The carboxy terminus of the beta amyloid protein is critical for the seeding of amyloid formation: implications for the pathogenesis of Alzheimer's disease, Biochemistry 32 (1993) 4693-4697.

[13] H. Naiki, K. Nakakuki, First-order kinetic model of Alzheimer's beta-amyloid fibril extension in vitro, Lab. Invest. 74 (1996) 374-383.

[14] M.P. Lambert, A.K. Barlow, B.A. Chromy, C. Edwards, R. Freed, M. Liosatos, T.E. Morgan, I. Rozovsky, B. Trommer, K.L. Viola, P. Wals, C. Zhang, C.E. Finch, G.A. Krafft, W.L. Klein, Diffusible, nonfibrillar ligands derived from Abeta1-42 are potent central nervous system neurotoxins, Proc Natl Acad Sci U S A 95 (1998) 6448-6453.

[15] R. Kayed, E. Head, J.L. Thompson, T.M. McIntire, S.C. Milton, C.W. Cotman, C.G. Glabe, Common structure of soluble amyloid oligomers implies common mechanism of pathogenesis, Science 300 (2003) 486-489.

[16] H.D. Nguyen, C.K. Hall, Molecular dynamics simulations of spontaneous fibril formation by random-coil peptides, Proc Natl Acad Sci U S A 101

(2004) 16180-16185.

[17] S. Lesne, M.T. Koh, L. Kotilinek, R. Kayed, C.G. Glabe, A. Yang, M. Gallagher, K.H. Ashe, A specific amyloid-beta protein assembly in the brain impairs memory, Nature 440 (2006) 352-357.

[18] C.G. Glabe, Conformation-dependent antibodies target diseases of protein misfolding, Trends Biochem Sci 29 (2004) 542-547.

[19] Y.M. Kuo, M.R. Emmerling, C. Vigo-Pelfrey, T.C. Kasunic, J.B. Kirkpatrick, G.H. Murdoch, M.J. Ball, A.E. Roher, Water-soluble Abeta (N-40, N-42) oligomers in normal and Alzheimer disease brains, J Biol Chem 271 (1996) 4077-4081.

[20] G. Bitan, M.D. Kirkitadze, A. Lomakin, S.S. Vollers, G.B. Benedek, D.B. Teplow, Amyloid beta -protein (Abeta) assembly: Abeta 40 and Abeta 42 oligomerize through distinct pathways, Proc Natl Acad Sci U S A 100 (2003) 330-335.

[21] J. Busciglio, A. Lorenzo, B.A. Yankner, Methodological variables in the assessment of beta amyloid neurotoxicity, Neurobiol Aging 13 (1992) 609-612.

[22] C. Geula, C.K. Wu, D. Saroff, A. Lorenzo, M. Yuan, B.A. Yankner, Aging renders the brain vulnerable to amyloid beta-protein neurotoxicity, Nat Med 4 (1998) 827-831.

[23] C. Haass, D.J. Selkoe, Soluble protein oligomers in neurodegeneration: lessons from the Alzheimer's amyloid beta-peptide, Nat Rev Mol Cell Biol 8 (2007) 101-112.

[24] C.A. McLean, R.A. Cherny, F.W. Fraser, S.J. Fuller, M.J. Smith, K. Beyreuther, A.I. Bush, C.L. Masters, Soluble pool of Abeta amyloid as a

determinant of severity of neurodegeneration in Alzheimer's disease, Ann Neurol 46 (1999) 860-866.

[25] J.P. Cleary, D.M. Walsh, J.J. Hofmeister, G.M. Shankar, M.A. Kuskowski, D.J. Selkoe, K.H. Ashe, Natural oligomers of the amyloid-beta protein specifically disrupt cognitive function, Nat Neurosci 8 (2005) 79-84.

[26] D.M. Walsh, D.J. Selkoe, Oligomers on the brain: the emerging role of soluble protein aggregates in neurodegeneration, Protein Pept Lett 11 (2004) 213-228.

[27] G.M. Shankar, S. Li, T.H. Mehta, A. Garcia-Munoz, N.E. Shepardson, I. Smith, F.M. Brett, M.A. Farrell, M.J. Rowan, C.A. Lemere, C.M. Regan, D.M. Walsh, B.L. Sabatini, D.J. Selkoe, Amyloid-beta protein dimers isolated directly from Alzheimer's brains impair synaptic plasticity and memory, Nat Med 14 (2008) 837-842.

[28] M.L. Giuffrida, F. Caraci, B. Pignataro, S. Cataldo, P. De Bona, V. Bruno, G. Molinaro, G. Pappalardo, A. Messina, A. Palmigiano, D. Garozzo, F. Nicoletti, E. Rizzarelli, A. Copani, Beta-amyloid monomers are neuroprotective, J Neurosci 29 (2009) 10582-10587.

[29] D.H. Small, S.S. Mok, J.C. Bornstein, Alzheimer's disease and Abeta toxicity: from top to bottom, Nat Rev Neurosci 2 (2001) 595-598.

[30] Y. Verdier, B. Penke, Binding sites of amyloid beta-peptide in cell plasma membrane and implications for Alzheimer's disease, Curr Protein Pept Sci 5 (2004) 19-31.

[31] R. Deane, Z. Wu, A. Sagare, J. Davis, S. Du Yan, K. Hamm, F. Xu, M. Parisi, B. LaRue, H.W. Hu, P. Spijkers, H. Guo, X. Song, P.J. Lenting, W.E. Van Nostrand, B.V. Zlokovic, LRP/amyloid beta-peptide interaction

mediates differential brain efflux of Abeta isoforms, Neuron 43 (2004) 333-344.

[32] H.Y. Wang, D.H. Lee, M.R. D'Andrea, P.A. Peterson, R.P. Shank, A.B. Reitz, beta-Amyloid(1-42) binds to alpha7 nicotinic acetylcholine receptor with high affinity. Implications for Alzheimer's disease pathology, J Biol Chem 275 (2000) 5626-5632.

[33] M. Yaar, S. Zhai, P.F. Pilch, S.M. Doyle, P.B. Eisenhauer, R.E. Fine, B.A. Gilchrest, Binding of beta-amyloid to the p75 neurotrophin receptor induces apoptosis. A possible mechanism for Alzheimer's disease, J Clin Invest 100 (1997) 2333-2340.

[34] S. Du Yan, H. Zhu, J. Fu, S.F. Yan, A. Roher, W.W. Tourtellotte, T. Rajavashisth, X. Chen, G.C. Godman, D. Stern, A.M. Schmidt, Amyloid-beta peptide-receptor for advanced glycation endproduct interaction elicits neuronal expression of macrophage-colony stimulating factor: a proinflammatory pathway in Alzheimer disease, Proc Natl Acad Sci U S A 94 (1997) 5296-5301.

[35] D.H. Small, D. Maksel, M.L. Kerr, J. Ng, X. Hou, C. Chu, H. Mehrani, S. Unabia, M.F. Azari, R. Loiacono, M.I. Aguilar, M. Chebib, The beta-amyloid protein of Alzheimer's disease binds to membrane lipids but does not bind to the alpha7 nicotinic acetylcholine receptor, J Neurochem 101 (2007) 1527-1538.

[36] O. Simakova, N.J. Arispe, The cell-selective neurotoxicity of the Alzheimer's Abeta peptide is determined by surface phosphatidylserine and cytosolic ATP levels. Membrane binding is required for Abeta toxicity, J Neurosci 27 (2007) 13719-13729.

[37] T. Kanekiyo, G. Bu, Receptor-associated protein interacts with amyloid-beta peptide and promotes its cellular uptake, J Biol Chem 284 (2009) 33352-33359.

[38] U. Kulandaivelu, V.G. Padmini, K. Suneetha, B. Shireesha, J.V. Vidyasagar, T.R. Rao, N.J. K, A. Basu, V. Jayaprakash, Synthesis, antimicrobial and anticancer activity of new thiosemicarbazone derivatives, Arch Pharm (Weinheim) 344 (2011) 84-90.

[39] C.H. Davis, M.L. Berkowitz, Structure of the amyloid-beta (1-42) monomer absorbed to model phospholipid bilayers: a molecular dynamics study, J Phys Chem B 113 (2009) 14480-14486.

[40] N. Arispe, E. Rojas, H.B. Pollard, Alzheimer disease amyloid beta protein forms calcium channels in bilayer membranes: blockade by tromethamine and aluminum, Proc Natl Acad Sci U S A 90 (1993) 567-571.

[41] B.L. Kagan, R. Azimov, R. Azimova, Amyloid peptide channels, J Membr Biol 202 (2004) 1-10.

[42] R. Lal, H. Lin, A.P. Quist, Amyloid beta ion channel: 3D structure and relevance to amyloid channel paradigm, Biochim Biophys Acta 1768 (2007) 1966-1975.

[43] L.M. Jungbauer, C. Yu, K.J. Laxton, M.J. LaDu, Preparation of fluorescently-labeled amyloid-beta peptide assemblies: the effect of fluorophore conjugation on structure and function, J Mol Recognit 22 (2009) 403-413.

[44] A.M. Cataldo, D.J. Hamilton, R.A. Nixon, Lysosomal abnormalities in degenerating neurons link neuronal compromise to senile plaque

development in Alzheimer disease, Brain Res 640 (1994) 68-80.

[45] C. Yu, E. Nwabuisi-Heath, K. Laxton, M.J. Ladu, Endocytic pathways mediating oligomeric Abeta42 neurotoxicity, Mol Neurodegener 5 (2010) 19.

[46] K.K. Kandimalla, O.G. Scott, S. Fulzele, M.W. Davidson, J.F. Poduslo, Mechanism of neuronal versus endothelial cell uptake of Alzheimer's disease amyloid beta protein, PLoS One 4 (2009) e4627.

[47] M.K. Lakshmana, W. Araki, T. Tabira, Amyloid beta peptide binds a novel death-inducing protein, AB-DIP, Faseb J 19 (2005) 1362-1364.

[48] L. Tillement, L. Lecanu, W. Yao, J. Greeson, V. Papadopoulos, The spirostenol (22R, 25R)-20alpha-spirost-5-en-3beta-yl hexanoate blocks mitochondrial uptake of Abeta in neuronal cells and prevents Abeta-induced impairment of mitochondrial function, Steroids 71 (2006) 725-735.

[49] C.A. Hansson Petersen, N. Alikhani, H. Behbahani, B. Wiehager, P.F. Pavlov, I. Alafuzoff, V. Leinonen, A. Ito, B. Winblad, E. Glaser, M. Ankarcrona, The amyloid beta-peptide is imported into mitochondria via the TOM import machinery and localized to mitochondrial cristae, Proc Natl Acad Sci U S A 105 (2008) 13145-13150.

[50] S.D. Yan, J. Fu, C. Soto, X. Chen, H. Zhu, F. Al-Mohanna, K. Collison, A. Zhu, E. Stern, T. Saido, M. Tohyama, S. Ogawa, A. Roher, D. Stern, An intracellular protein that binds amyloid-beta peptide and mediates neurotoxicity in Alzheimer's disease, Nature 389 (1997) 689-695.

[51] Y. Murakami, I. Ohsawa, T. Kasahara, S. Ohta, Cytoprotective role of mitochondrial amyloid beta peptide-binding alcohol dehydrogenase

against a cytotoxic aldehyde, Neurobiol Aging 30 (2009) 325-329.

[52] P.I. Moreira, M.S. Santos, A. Moreno, A.C. Rego, C. Oliveira, Effect of amyloid beta-peptide on permeability transition pore: a comparative study, J Neurosci Res 69 (2002) 257-267.

[53] P. Singh, S. Suman, S. Chandna, T.K. Das, Possible role of amyloid-beta, adenine nucleotide translocase and cyclophilin-D interaction in mitochondrial dysfunction of Alzheimer's disease, Bioinformation 3 (2009) 440-445.

[54] L. Tillement, L. Lecanu, V. Papadopoulos, Alzheimer's disease: effects of beta-amyloid on mitochondria, Mitochondrion 11 (2011) 13-21.

[55] Y.P. Li, A.F. Bushnell, C.M. Lee, L.S. Perlmutter, S.K. Wong, Beta-amyloid induces apoptosis in human-derived neurotypic SH-SY5Y cells, Brain Res 738 (1996) 196-204.

[56] S. Estus, H.M. Tucker, C. van Rooyen, S. Wright, E.F. Brigham, M. Wogulis, R.E. Rydel, Aggregated amyloid-beta protein induces cortical neuronal apoptosis and concomitant "apoptotic" pattern of gene induction, J Neurosci 17 (1997) 7736-7745.

[57] T.T. Rohn, R.A. Rissman, E. Head, C.W. Cotman, Caspase Activation in the Alzheimer's Disease Brain: Tortuous and Torturous, Drug News Perspect 15 (2002) 549-557.

[58] N.A. Thornberry, Y. Lazebnik, Caspases: enemies within, Science 281 (1998) 1312-1316.

[59] C. Behl, Apoptosis and Alzheimer's disease, J Neural Transm 107 (2000) 1325-1344.

[60] S. Shimohama, Apoptosis in Alzheimer's disease--an update, Apoptosis 5

(2000) 9-16.

[61] P. Li, D. Nijhawan, I. Budihardjo, S.M. Srinivasula, M. Ahmad, E.S. Alnemri, X. Wang, Cytochrome c and dATP-dependent formation of Apaf-1/caspase-9 complex initiates an apoptotic protease cascade, Cell 91 (1997) 479-489.

[62] Y. Imai, T. Kimura, A. Murakami, N. Yajima, K. Sakamaki, S. Yonehara, The CED-4-homologous protein FLASH is involved in Fas-mediated activation of caspase-8 during apoptosis, Nature 398 (1999) 777-785.

[63] K.M. Boatright, G.S. Salvesen, Mechanisms of caspase activation, Curr Opin Cell Biol 15 (2003) 725-731.

[64] D.T. Loo, A. Copani, C.J. Pike, E.R. Whittemore, A.J. Walencewicz, C.W. Cotman, Apoptosis is induced by beta-amyloid in cultured central nervous system neurons, Proc Natl Acad Sci U S A 90 (1993) 7951-7955.

[65] H.S. Kim, J.H. Lee, J.P. Lee, E.M. Kim, K.A. Chang, C.H. Park, S.J. Jeong, M.C. Wittendorp, J.H. Seo, S.H. Choi, Y.H. Suh, Amyloid beta peptide induces cytochrome C release from isolated mitochondria, Neuroreport 13 (2002) 1989-1993.

[66] J. Harada, M. Sugimoto, Activation of caspase-3 in beta-amyloid-induced apoptosis of cultured rat cortical neurons, Brain Res 842 (1999) 311-323.

[67] M. Yao, T.V. Nguyen, C.J. Pike, Beta-amyloid-induced neuronal apoptosis involves c-Jun N-terminal kinase-dependent downregulation of Bcl-w, J Neurosci 25 (2005) 1149-1158.

[68] A. Demuro, I. Parker, G.E. Stutzmann, Calcium signaling and amyloid

toxicity in Alzheimer disease, J Biol Chem 285 (2010) 12463-12468.

[69] K. Jomova, D. Vondrakova, M. Lawson, M. Valko, Metals, oxidative stress and neurodegenerative disorders, Mol Cell Biochem 345 (2010) 91-104.

[70] Q. Zhang, J.T. Yu, Q.X. Zhu, W. Zhang, Z.C. Wu, D. Miao, L. Tan, Complement receptor 1 polymorphisms and risk of late-onset Alzheimer's disease, Brain Res 1348 (2010) 216-221.

[71] C.I. Stains, K. Mondal, I. Ghosh, Molecules that target beta-amyloid, ChemMedChem 2 (2007) 1674-1692.

[72] H. Wegele, S.K. Wandinger, A.B. Schmid, J. Reinstein, J. Buchner, Substrate transfer from the chaperone Hsp70 to Hsp90, J Mol Biol 356 (2006) 802-811.

[73] F.U. Hartl, M. Hayer-Hartl, Molecular chaperones in the cytosol: from nascent chain to folded protein, Science 295 (2002) 1852-1858.

[74] A. Golabek, M.A. Marques, M. Lalowski, T. Wisniewski, Amyloid beta binding proteins in vitro and in normal human cerebrospinal fluid, Neurosci Lett 191 (1995) 79-82.

[75] Y.C. Kudva, H.J. Hiddinga, P.C. Butler, C.S. Mueske, N.L. Eberhardt, Small heat shock proteins inhibit in vitro A beta(1-42) amyloidogenesis, FEBS Lett 416 (1997) 117-121.

[76] S. Lee, K. Carson, A. Rice-Ficht, T. Good, Small heat shock proteins differentially affect Abeta aggregation and toxicity, Biochem Biophys Res Commun 347 (2006) 527-533.

[77] S. Lee, K. Carson, A. Rice-Ficht, T. Good, Hsp20, a novel alpha-crystallin, prevents Abeta fibril formation and toxicity, Protein Sci 14 (2005) 593-601.

[78] V. Fonte, V. Kapulkin, A. Taft, A. Fluet, D. Friedman, C.D. Link, Interaction of intracellular beta amyloid peptide with chaperone proteins, Proc Natl Acad Sci U S A 99 (2002) 9439-9444.

[79] V. Fonte, D.R. Kipp, J. Yerg, 3rd, D. Merin, M. Forrestal, E. Wagner, C.M. Roberts, C.D. Link, Suppression of in vivo beta-amyloid peptide toxicity by overexpression of the HSP-16.2 small chaperone protein, J Biol Chem 283 (2008) 784-791.

[80] T. Oda, P. Wals, H.H. Osterburg, S.A. Johnson, G.M. Pasinetti, T.E. Morgan, I. Rozovsky, W.B. Stine, S.W. Snyder, T.F. Holzman, et al., Clusterin (apoJ) alters the aggregation of amyloid beta-peptide (A beta 1-42) and forms slowly sedimenting A beta complexes that cause oxidative stress, Exp Neurol 136 (1995) 22-31.

[81] A.M. Manelli, W.B. Stine, L.J. Van Eldik, M.J. LaDu, ApoE and Abeta1-42 interactions: effects of isoform and conformation on structure and function, J Mol Neurosci 23 (2004) 235-246.

[82] C.G. Evans, S. Wisen, J.E. Gestwicki, Heat shock proteins 70 and 90 inhibit early stages of amyloid beta-(1-42) aggregation in vitro, J Biol Chem 281 (2006) 33182-33191.

[83] M.M. Wilhelmus, W.C. Boelens, I. Otte-Holler, B. Kamps, B. Kusters, M.L. Maat-Schieman, R.M. de Waal, M.M. Verbeek, Small heat shock protein HspB8: its distribution in Alzheimer's disease brains and its inhibition of amyloid-beta protein aggregation and cerebrovascular amyloid-beta toxicity, Acta Neuropathol 111 (2006) 139-149.

[84] G.J. Stege, K. Renkawek, P.S. Overkamp, P. Verschuure, A.F. van Rijk, A. Reijnen-Aalbers, W.C. Boelens, G.J. Bosman, W.W. de Jong, The

molecular chaperone alphaB-crystallin enhances amyloid beta neurotoxicity, Biochem Biophys Res Commun 262 (1999) 152-156.

[85] M. Folin, S. Baiguera, D. Guidolin, R. Di Liddo, C. Grandi, E. De Carlo, G.G. Nussdorfer, P.P. Parnigotto, Apolipoprotein-E modulates the cytotoxic effect of beta-amyloid on rat brain endothelium in an isoform-dependent specific manner, Int J Mol Med 17 (2006) 821-826.

[86] M.V. Aksenova, M.Y. Aksenov, D.A. Butterfield, J.M. Carney, alpha-1-antichymotrypsin interaction with A beta (1-40) inhibits fibril formation but does not affect the peptide toxicity, Neurosci Lett 211 (1996) 45-48.

[87] J.J. Yerbury, S. Poon, S. Meehan, B. Thompson, J.R. Kumita, C.M. Dobson, M.R. Wilson, The extracellular chaperone clusterin influences amyloid formation and toxicity by interacting with prefibrillar structures, Faseb J 21 (2007) 2312-2322.

[88] M. Necula, R. Kayed, S. Milton, C.G. Glabe, Small molecule inhibitors of aggregation indicate that amyloid beta oligomerization and fibrillization pathways are independent and distinct, J Biol Chem 282 (2007) 10311-10324.

[89] F. Yang, G.P. Lim, A.N. Begum, O.J. Ubeda, M.R. Simmons, S.S. Ambegaokar, P.P. Chen, R. Kayed, C.G. Glabe, S.A. Frautschy, G.M. Cole, Curcumin inhibits formation of amyloid beta oligomers and fibrils, binds plaques, and reduces amyloid in vivo, J Biol Chem 280 (2005) 5892-5901.

[90] S.J. Pollack, Sadler, II, S.R. Hawtin, V.J. Tailor, M.S. Shearman, Sulfonated dyes attenuate the toxic effects of beta-amyloid in a structure-specific fashion, Neurosci Lett 197 (1995) 211-214.

[91] V.M. Lee, Amyloid binding ligands as Alzheimer's disease therapies, Neurobiol Aging 23 (2002) 1039-1042.

[92] A. Aggeli, M. Bell, N. Boden, J.N. Keen, P.F. Knowles, T.C. McLeish, M. Pitkeathly, S.E. Radford, Responsive gels formed by the spontaneous self-assembly of peptides into polymeric beta-sheet tapes, Nature 386 (1997) 259-262.

[93] E. Gazit, A possible role for pi-stacking in the self-assembly of amyloid fibrils, Faseb J 16 (2002) 77-83.

[94] E. Gazit, Mechanistic studies of the process of amyloid fibrils formation by the use of peptide fragments and analogues: implications for the design of fibrillization inhibitors, Curr Med Chem 9 (2002) 1725-1735.

[95] G.G. Tartaglia, A. Cavalli, R. Pellarin, A. Caflisch, The role of aromaticity, exposed surface, and dipole moment in determining protein aggregation rates, Protein Sci 13 (2004) 1939-1941.

[96] Y. Porat, A. Abramowitz, E. Gazit, Inhibition of amyloid fibril formation by polyphenols: structural similarity and aromatic interactions as a common inhibition mechanism, Chem Biol Drug Des 67 (2006) 27-37.

[97] J.P. Spencer, Flavonoids: modulators of brain function?, Br J Nutr 99 E Suppl 1 (2008) ES60-77.

[98] D. Bagchi, O.R. Carryl, M.X. Tran, M. Bagchi, A. Garg, M.M. Milnes, C.B. Williams, J. Balmoori, D.J. Bagchi, S. Mitra, S.J. Stohs, Acute and chronic stress-induced oxidative gastrointestinal mucosal injury in rats and protection by bismuth subsalicylate, Mol Cell Biochem 196 (1999) 109-116.

[99] Y. Yamamoto, R.B. Gaynor, Therapeutic potential of inhibition of the NF-

kappaB pathway in the treatment of inflammation and cancer, J Clin Invest 107 (2001) 135-142.

[100] T.P. Cushnie, A.J. Lamb, Antimicrobial activity of flavonoids, Int J Antimicrob Agents 26 (2005) 343-356.

[101] D. Commenges, V. Scotet, S. Renaud, H. Jacqmin-Gadda, P. Barberger-Gateau, J.F. Dartigues, Intake of flavonoids and risk of dementia, Eur J Epidemiol 16 (2000) 357-363.

[102] Z. Yao, K. Drieu, V. Papadopoulos, The Ginkgo biloba extract EGb 761 rescues the PC12 neuronal cells from beta-amyloid-induced cell death by inhibiting the formation of beta-amyloid-derived diffusible neurotoxic ligands, Brain Res 889 (2001) 181-190.

[103] Y. Luo, J.V. Smith, V. Paramasivam, A. Burdick, K.J. Curry, J.P. Buford, I. Khan, W.J. Netzer, H. Xu, P. Butko, Inhibition of amyloid-beta aggregation and caspase-3 activation by the Ginkgo biloba extract EGb761, Proc Natl Acad Sci U S A 99 (2002) 12197-12202.

[104] C.N. Wang, C.W. Chi, Y.L. Lin, C.F. Chen, Y.J. Shiao, The neuroprotective effects of phytoestrogens on amyloid beta protein-induced toxicity are mediated by abrogating the activation of caspase cascade in rat cortical neurons, J Biol Chem 276 (2001) 5287-5295.

[105] J.H. Lu, M.T. Ardah, S.S. Durairajan, L.F. Liu, L.X. Xie, W.F. Fong, M.Y. Hasan, J.D. Huang, O.M. El-Agnaf, M. Li, Baicalein Inhibits Formation of alpha-Synuclein Oligomers within Living Cells and Prevents Abeta Peptide Fibrillation and Oligomerisation, Chembiochem (2011).

[106] C. Ramassamy, Emerging role of polyphenolic compounds in the treatment of neurodegenerative diseases: a review of their intracellular

targets, Eur J Pharmacol 545 (2006) 51-64.

[107] M. Shahnawaz, A. Thapa, I.S. Park, Stable activity of a deubiquitylating enzyme (Usp2-cc) in the presence of high concentrations of urea and its application to purify aggregation-prone peptides, Biochem Biophys Res Commun 359 (2007) 801-805.

[108] B.A. Chromy, R.J. Nowak, M.P. Lambert, K.L. Viola, L. Chang, P.T. Velasco, B.W. Jones, S.J. Fernandez, P.N. Lacor, P. Horowitz, C.E. Finch, G.A. Krafft, W.L. Klein, Self-assembly of Abeta(1-42) into globular neurotoxins, Biochemistry 42 (2003) 12749-12760.

[109] P. Karki, C. Seong, J.E. Kim, K. Hur, S.Y. Shin, J.S. Lee, B. Cho, I.S. Park, Intracellular K(+) inhibits apoptosis by suppressing the Apaf-1 apoptosome formation and subsequent downstream pathways but not cytochrome c release, Cell Death Differ 14 (2007) 2068-2075.

[110] K. Hsiao, P. Chapman, S. Nilsen, C. Eckman, Y. Harigaya, S. Younkin, F. Yang, G. Cole, Correlative memory deficits, Abeta elevation, and amyloid plaques in transgenic mice, Science 274 (1996) 99-102.

[111] P. Karki, G.R. Dahal, I.S. Park, Both dimerization and interdomain processing are essential for caspase-4 activation, Biochem Biophys Res Commun 356 (2007) 1056-1061.

[112] H. Naiki, K. Hasegawa, I. Yamaguchi, H. Nakamura, F. Gejyo, K. Nakakuki, Apolipoprotein E and antioxidants have different mechanisms of inhibiting Alzheimer's beta-amyloid fibril formation in vitro, Biochemistry 37 (1998) 17882-17889.

[113] M.D. Kirkitadze, M.M. Condron, D.B. Teplow, Identification and characterization of key kinetic intermediates in amyloid beta-protein

fibrillogenesis, J Mol Biol 312 (2001) 1103-1119.

[114] M.A. Moss, N.H. Varvel, M.R. Nichols, D.K. Reed, T.L. Rosenberry, Nordihydroguaiaretic acid does not disaggregate beta-amyloid(1-40) protofibrils but does inhibit growth arising from direct protofibril association, Mol Pharmacol 66 (2004) 592-600.

[115] K. Zou, J.S. Gong, K. Yanagisawa, M. Michikawa, A novel function of monomeric amyloid beta-protein serving as an antioxidant molecule against metal-induced oxidative damage, J Neurosci 22 (2002) 4833-4841.

[116] M.L. Liu, S.T. Hong, Early phase of amyloid beta42-induced cytotoxicity in neuronal cells is associated with vacuole formation and enhancement of exocytosis, Exp Mol Med 37 (2005) 559-566.

[117] T.L. Yue, C. Wang, A.M. Romanic, K. Kikly, P. Keller, W.E. DeWolf, Jr., T.K. Hart, H.C. Thomas, B. Storer, J.L. Gu, X. Wang, G.Z. Feuerstein, Staurosporine-induced apoptosis in cardiomyocytes: A potential role of caspase-3, J Mol Cell Cardiol 30 (1998) 495-507.

[118] D. Tang, J.M. Lahti, V.J. Kidd, Caspase-8 activation and bid cleavage contribute to MCF7 cellular execution in a caspase-3-dependent manner during staurosporine-mediated apoptosis, J Biol Chem 275 (2000) 9303-9307.

[119] M.J. Sculley, J.F. Morrison, W.W. Cleland, Slow-binding inhibition: the general case, Biochim Biophys Acta 1298 (1996) 78-86.

[120] T.T. Rohn, The role of caspases in Alzheimer's disease; potential novel therapeutic opportunities, Apoptosis 15 (2010) 1403-1409.

[121] V. Rangachari, B.D. Moore, D.K. Reed, L.K. Sonoda, A.W. Bridges, E.

Conboy, D. Hartigan, T.L. Rosenberry, Amyloid-beta(1-42) Rapidly Forms Protofibrils and Oligomers by Distinct Pathways in Low Concentrations of Sodium Dodecylsulfate, Biochemistry (2007).

[122] M.D. Kirkitadze, M.M. Condron, D.B. Teplow, Identification and characterization of key kinetic intermediates in amyloid beta-protein fibrillogenesis, J. Mol. Biol. 312 (2001) 1103-1119.

[123] F.C. Dehle, H. Ecroyd, I.F. Musgrave, J.A. Carver, alphaB-Crystallin inhibits the cell toxicity associated with amyloid fibril formation by kappa-casein and the amyloid-beta peptide, Cell Stress Chaperones 15 (2010) 1013-1026.

[124] A.R. Ladiwala, J.C. Lin, S.S. Bale, A.M. Marcelino-Cruz, M. Bhattacharya, J.S. Dordick, P.M. Tessier, Resveratrol selectively remodels soluble oligomers and fibrils of amyloid Abeta into off-pathway conformers, J Biol Chem 285 (2010) 24228-24237.

[125] M. Wogulis, S. Wright, D. Cunningham, T. Chilcote, K. Powell, R.E. Rydel, Nucleation-dependent polymerization is an essential component of amyloid-mediated neuronal cell death, J Neurosci 25 (2005) 1071-1080.

[126] J.T. Zhu, R.C. Choi, G.K. Chu, A.W. Cheung, Q.T. Gao, J. Li, Z.Y. Jiang, T.T. Dong, K.W. Tsim, Flavonoids possess neuroprotective effects on cultured pheochromocytoma PC12 cells: a comparison of different flavonoids in activating estrogenic effect and in preventing beta-amyloid-induced cell death, J Agric Food Chem 55 (2007) 2438-2445.

[127] M. Masuda, N. Suzuki, S. Taniguchi, T. Oikawa, T. Nonaka, T. Iwatsubo, S. Hisanaga, M. Goedert, M. Hasegawa, Small molecule inhibitors of alpha-synuclein filament assembly, Biochemistry 45 (2006) 6085-6094.

[128] D.M. Walsh, D.M. Hartley, Y. Kusumoto, Y. Fezoui, M.M. Condron, A. Lomakin, G.B. Benedek, D.J. Selkoe, D.B. Teplow, Amyloid beta-protein fibrillogenesis. Structure and biological activity of protofibrillar intermediates, J Biol Chem 274 (1999) 25945-25952.

[129] A. Thapa, E.R. Woo, E.Y. Chi, M.G. Sharoar, H.G. Jin, S.Y. Shin, I.S. Park, Biflavonoids Are Superior to Monoflavonoids in Inhibiting Amyloid-beta Toxicity and Fibrillogenesis via Accumulation of Nontoxic Oligomer-like Structures, Biochemistry 50 (2011) 2445-2455.

[130] D.H. Shin, Y.C. Bae, J.S. Kim-Han, J.H. Lee, I.Y. Choi, K.H. Son, S.S. Kang, W.K. Kim, B.H. Han, Polyphenol amentoflavone affords neuroprotection against neonatal hypoxic-ischemic brain damage via multiple mechanisms, J Neurochem 96 (2006) 561-572.

[131] C.W. Lee, H.J. Choi, H.S. Kim, D.H. Kim, I.S. Chang, H.T. Moon, S.Y. Lee, W.K. Oh, E.R. Woo, Biflavonoids isolated from Selaginella tamariscina regulate the expression of matrix metalloproteinase in human skin fibroblasts, Bioorg Med Chem 16 (2008) 732-738.

[132] K. Ono, Y. Yoshiike, A. Takashima, K. Hasegawa, H. Naiki, M. Yamada, Potent anti-amyloidogenic and fibril-destabilizing effects of polyphenols in vitro: implications for the prevention and therapeutics of Alzheimer's disease, J Neurochem 87 (2003) 172-181.

[133] Y. Porat, Y. Mazor, S. Efrat, E. Gazit, Inhibition of islet amyloid polypeptide fibril formation: a potential role for heteroaromatic interactions, Biochemistry 43 (2004) 14454-14462.

[134] Y. Nakagami, S. Nishimura, T. Murasugi, I. Kaneko, M. Meguro, S. Marumoto, H. Kogen, K. Koyama, T. Oda, A novel beta-sheet breaker,

RS-0406, reverses amyloid beta-induced cytotoxicity and impairment of long-term potentiation in vitro, Br J Pharmacol 137 (2002) 676-682.

V. ABBREVIATIONS

AβOs; oligomers composed of 15–20 monomers

ABAD; β-amyloid binding alcohol dehydrogenase

AB-DIP; Aβ-related death-inducing protein

Ac-DEVD-AMC; N-acetyl Asp-Glu-Val-Asp-amino methyl coumarin

ACE; Aβ treated cell extract

Ac-LEHD-AMC; N-acetyl Leu-Glu-His-Asp-amino methyl coumarin

AD; Alzheimer's disease

ADDLs; Aβ -derived diffusible ligands

Apo E; apolipoprotein E

ApoJ; apolipoprotein J

APP; amyloid precursor protein

Aβ; β-amyloid

CAB; Caspase assay buffer

CD; circular dichroism

DISC; death inducing signaling complex

DMEM; Dulbecco's modified Eagles medium

DTT; Dithiothreitol

ER; endoplasmic reticulum

ERAB; endoplasmic reticulum amyloid β-peptide-binding protein

fAβ; fibrilar form of Aβ

FBS; fetal bovine serum

HCE; healthy cell extract

HNE; hydroxy-2-nonenal

Hsp; heat shocks protein

LPL; lipoprotein lipase

MPTP; membrane permeability transition pore

MTT; 3-(4,5-dimethylthiazol-2-yl)-2,5-diphenyl tetrazolium bromide

PMSF; phenylmethanesulphonylchloride

PVDF; poly vinylidene difluoride

RAP; receptor associated protein

RFU; relative fluorescence unit

ROS; reactive oxygen species

SDS-PAGE; sodium dodecylsulfate-polyacrylamide gel electrophoresis

sHsp; small heat shocks protein

TEM; transmission electron microscopy

ThT; thioflavin T

TIM; translocase of the inner membrane

TOM; translocase of the outer membrane

Z-VAD-FMK; benzyloxycarbonyl-Val-Ala-Asp -fluoromethylketone

VI. ABSTRACT

Identification and characterization of amyloid beta interacting proteins

Md. Golam Sharoar
Advisor: Prof. Il-Seon Park
Department of Biomaterials
Graduate School of Chosun University

Amyloid β (Aβ) is a major constituent of diffuse plaques in Alzheimer's disease. The peptide has been known to cause cell death through intra- and extracellular processes including apoptosis in which caspases are activated. The present study, however, identified a new interaction of Aβ peptide with caspase-9 and showed that the cytotoxic peptide also has an anti-apoptotic function. Extracellular Aβ42 decreased DEVDase activity and MTT reduction induced by staurosporine treatment. This was due to inhibitory effects of the peptide on the assembly of Apaf-1 apoptosome and consequent activation of caspase-9 and -3. Aβ42 was found to interact with the pro form of caspase-9 which prevents the recruitment of the caspase to the apoptosome. Aβ peptide also inhibited the enzyme activity of procaspase-9. The interaction was not detected with CARD-deleted caspase-9, implying the importance of the domain

in the interaction. Notably, the anti-apoptotic effect was robust in epithelial HeLa and osteosarcoma MG63 cells, while it was relatively weak in neuroblastoma SHSY5Y cells. Finally, the consequent of the interaction was found to form the caspase-9 inclusion body.

Aggregation of Aβ peptide is an important event in the development of the disease. An extracellular chaperone like protein, called maltose binding protein (MBP), was utilized to inhibit the assembly of the peptide. The protein found to be interacted to Aβ peptide at an earlier stage of assembly process and effectively inhibited the fibril formation at higher molar ratio to the peptide. MBP also blocked the transition of the peptide from monomeric random coil to secondary β-sheet structure. The consequences of inhibition, several intermediate Aβ species were accumulated. Interestingly, the accumulated oligomeric species were less toxic to the human neuroblastoma SH-SY5Y cells. The results suggested that MBP preferentially hinder the nucleation step of Aβ fibrilogenesis and modulated the peptide to non-toxic oligomeric conformation.

Further, the effect of a natural flavonoid, Keampferol-3-rhamnoside (K-3-rh), on Aβ42 aggregation and cyto-toxicity was investigated to better understand the assembly mechanism. The flavonoid was effective against Aβ mediated cytotoxicity in dose dependent manner. Anti-amyloidogenic properties of K-3-rh found to be efficient in inhibiting fibril formation, fibril extension, fibril disintegration and secondary structural transformation of the peptide. Several oligomeric structures were observed in presence of higher concentration of the compound. The data indicated that K-3-rh might be converted the aggregation pathway of Aβ peptid to form off-pathway oligomers.

VII. ACKNOWLEDGEMENTS

At first, I would like to express my sincere gratitude to my supervisor Prof. Il-Seon Park for his supervision, advice, guidance and training throughout the work. His help, advice, dedication and remarkable knowledge covering extraordinarily large areas of protein biochemistry have been invaluable for my thesis work. I would like to extend my sincere gratitude to Prof. Kyung-Soo Hahm, Prof. Song Yub Shin, Prof. Tae Hyoung Kim and Prof. Takbum Ohn for their valuable suggestion and support in various ways.

I reserve the deep note of appreciation to my previous supervisors Prof. M Abdul Khaleque and my teachers Prof. O.I. Joarder, Prof. Anil Chandra Deb, Prof. Bisawanath Shikhdar, Dr. Shahriar Zaman, Dr. Abu Reza, and Dr. Zennat Ferdousi for their contribution in my career.

I gratefully thank to my seniors Pratap, Arjun and Shahnawaz for their training at initial stage and immense support during my work and to my colleagues Vijay and Imam for their countless help. I wish to thank my friends, Dr. Robash, Dr. Jung Eun, Gopal, Jung-Woo, Young Hae and Ju-Young for their kindness that made my life in Korea much easier. All the members of Molecular and Cell Biology, Peptide Biochemistry, Peptide Engineering and Korea DNA Repair laboratory get warmest thanks giving me the possibility of sharing their working facilities.

Finally, I would like to thank my parents, my sisters and brothers, my wife and my son for their support and encouragement throughout my academic career.